



Supporting Information

The Fe₂(NO)₂ Diamond Core: A Unique Structural Motif In Non-Heme Iron–NO Chemistry

*Hai T. Dong, Amy L. Speelman, Claire E. Kozemchak, Debangsu Sil, Carsten Krebs, and Nicolai Lehnert**

ange_201911968_sm_miscellaneous_information.pdf

SUPPORTING INFORMATION**Table of Contents**

Experimental Section.	S3-5
UV-Vis spectra:	
Complex 1 vs. [Fe(TPA)(CH ₃ CN) ₂](OTf) ₂	S6
CoCp ₂ titration of complex 1 to form complex 2	S7
Solid state and solution IR spectra:	
Solid state IR of 1 with n.a.i., ¹⁵ NO, and ¹⁵ N ¹⁸ O	S8
Solid state IR of 2 with n.a.i., ¹⁵ NO, and ¹⁵ N ¹⁸ O	S9
Solid state IR spectra of 2 with n.a.i. and labeled ¹⁵ NO showing perfect overlap of the ligand region.....	S10
Reduction of 1 in solution	S11
Solid state IR of 3	S12
Solution IR of 3 and its reduction in solution to form the DNIC product	S13
Solid state IR of 1-BF₄	S14
Solution IR of 1-BF₄	S15
Cyclic voltammetry:	
Complex 1	S16
Complex 3	S17
EPR:	
Complex 1 in CH ₂ Cl ₂ and CH ₃ CN, in comparison with the solution IR spectra	S18
Complex 3 in CH ₂ Cl ₂ and CH ₃ CN.....	S19
Complex 1 in THF	S20
Complex 1 in MeOH	S21
Complex 1-BF₄ in CH ₂ Cl ₂ vs CH ₃ CN	S22
Complex 1-BF₄ in CH ₃ CN	S23
TOF HPLC-MS	
Complex 2 with n.a.i. NO	S24
Complex 2 with ¹⁵ NO.....	S25
NMR spectra:	
¹ H-NMR spectrum of coligand TPA.....	S26
¹ H-NMR spectrum of Complex 2	S27
¹ H-NMR spectrum of coligand BMPA-tBu ₂ PhOH	S28
Crystal Structure:	
Crystal structure of complex 1 and essential structural parameters.....	S29-39
Crystal structure of complex 2 and essential structural parameters.....	S40-50
Crystal structure of complex 3 and essential structural parameters.....	S51-64
DFT	
Optimized structures of complex 2 with BP86/TZVP and B3LYP/TZVP	S65-69
Optimized structures of complex 1 with OTf ⁻ and CH ₃ CN bound (hs and ls) using B3LYP*/TZVP	S70-73
Optimized structures of the hs and ls forms of 1red with OTf ⁻ bound using B3LYP*/TZVP.....	S74-75

SUPPORTING INFORMATION

Experimental Procedures

Reactions were generally performed using inert gas (Schlenk) techniques. All solvents were dried and freeze pump thawed to remove dioxygen and water. Preparation and handling of air sensitive materials was performed under a dinitrogen atmosphere in an MBraun glovebox, equipped with a circulating purifier ($O_2, H_2O < 0.1$ ppm). Nitric oxide (99.95%) was first passed through an Ascarite II column and then a -80 °C cold trap to remove higher nitrogen oxide impurities prior to use.

Infrared spectra of neat solid samples were obtained using PerkinElmer BX and GX and Bruker Alpha-E FTIR spectrometers. The IR spectra of solution samples were obtained in thin-layer solution cells equipped with CaF_2 windows. Gas IR spectra were obtained using a Pike Technologies short-path HT gas cell with 100 mm path length, equipped with CaF_2 windows, on the same instruments.

UV-Vis/Immersion probe spectra were obtained using an Analytic Jena Specord S600 UV-Vis spectrometer. Dip probe experiments used the same spectrometer, with a Hellma low-temperature immersion probe.

NMR spectra were recorded on a Varian Vnmrs 700 MHz instrument and referenced against residual solvent signals.

Cyclic voltammograms (CVs) were obtained on a CH instruments CHI660C electrochemical workstation using a three-component cell, consisting of a glassy carbon working electrode, a platinum auxiliary electrode, and a Ag wire pseudoreference electrode. CVs were recorded in 0.1 M tetrabutylammonium hexafluorophosphate in CH_2Cl_2 . Potentials were corrected to the Fc^+/Fc standard by independently measuring the ferrocenium/ferrocene couple under the same conditions ($Fc^+/Fc = 624$ mV vs. SHE).

IR Spectroelectrochemistry experiments were conducted using a LabOmak UF-SEC thin layer cell, with Pt mesh working and counter electrodes, and an Ag wire pseudoreference electrode.

Electron paramagnetic resonance spectra were recorded on a Bruker X-band EMX spectrometer equipped with Oxford Instruments liquid nitrogen and liquid helium flow cryostats. EPR spectra were typically obtained on frozen solutions using ~20 mW microwave power and 100 kHz field modulation with the amplitude set to 1 G. Sample concentrations were ~2 mM.

Mössbauer spectra were recorded on a spectrometer from SEECO (Edina, MN) equipped with a Janis SVT-400 variable-temperature cryostat. The reported isomer shift is relative to the centroid of the spectrum of α-iron metal at room temperature. Simulations of the Mössbauer spectra were carried out using the WMOSS spectral analysis software from SEECO (www.wmoss.org; Edina, MN).

Elemental analyses were conducted by Atlantic Microlabs (Norcross, GA).

Mass spectrometry experiments were conducted on an Agilent 6230 TOF HPLC-MS with manual injection. Compounds were dissolved in CH_2Cl_2 and then injected directly into the instrument.

Structure Determination: Brown plates of complex **1** were grown from an acetonitrile/diethyl ether solution of the compound at 22 deg. C. A crystal of dimensions 0.20 x 0.14 x 0.08 mm was mounted on a Rigaku AFC10K Saturn 944+ CCD-based X-ray diffractometer equipped with a low temperature device and a Micromax-007HF Cu-target micro-focus rotating anode ($\lambda = 1.54187$ Å) operated at 1.2 kW power (40 kV, 30 mA). The X-ray intensities were measured at 85(1) K with the detector placed at a distance of 42.00 mm from the crystal. A total of 3808 images were collected with an oscillation width of 1.0° in ω . The exposure times were 2 sec. for the low angle images, 12 sec. for high angle. The integration of the data yielded a total of 35,038 reflections to a maximum 2θ value of 136.48° of which 4698 were independent and 4600 were greater than $2\sigma(I)$. The final cell constants (Table S2) were based on the xyz centroids of 18,779 reflections above 10 $\sigma(I)$. Analysis of the data showed negligible decay during data collection; the data were processed with CrystalClear 2.0 and corrected for absorption.¹ The structure was solved and refined with the Bruker SHELXTL (version 2018/3) software package, using the space group P1bar with Z = 2 for the formula $C_{20}H_{18}N_5O_7F_6S_2Fe$.² All non-hydrogen atoms were refined anisotropically with the hydrogen atoms placed in idealized positions. Full matrix least-squares refinement based on F2 converged at R1 = 0.0311 and wR2 = 0.0843 [based on $I > 2\sigma(I)$], R1 = 0.0315 and wR2 = 0.0846 for all data. Additional details are presented in Table S2 and are given as Supporting Information in a CIF file. Acknowledgement is made for funding from NSF grant CHE-0840456 for X-ray instrumentation.

Purple blocks of complex **2** were grown from an acetonitrile/diethyl ether solution of the compound at -33 deg. C. A crystal of dimensions 0.12 x 0.10 x 0.10 mm was mounted on a Rigaku AFC10K Saturn 944+ CCD-based X-ray diffractometer equipped with a low temperature device and a Micromax-007HF Cu-target micro-focus rotating anode ($\lambda = 1.54187$ Å) operated at 1.2 kW power (40 kV, 30 mA). The X-ray intensities were measured at 85(1) K with the detector placed at a distance of 42.00 mm from the crystal. A total of

SUPPORTING INFORMATION

2028 images were collected with an oscillation width of 1.0° in ω . The exposure times were 1 sec. for the low angle images, 3 sec. for high angle. Rigaku d*trek images were exported to CrysAlisPro for processing and corrected for absorption.³ The integration of the data yielded a total of 31,405 reflections to a maximum 2θ value of 138.32° of which 3875 were independent and 3769 were greater than $2\sigma(I)$. The final cell constants (Table S9) were based on the xyz centroids of 18,500 reflections above $10\sigma(I)$. Analysis of the data showed negligible decay during data collection. The structure was solved and refined with the Bruker SHELXTL (version 2016/6) software package, using the space group P2(1)/c with Z = 2 for the formula $C_{38}H_{36}F_6Fe_2N_{10}O_8S_2$. All non-hydrogen atoms were refined anisotropically with the hydrogen atoms placed in idealized positions. Full matrix least-squares refinement based on F2 converged at R1 = 0.0314 and wR2 = 0.0847 [based on $I > 2\sigma(I)$], R1 = 0.0323 and wR2 = 0.0856 for all data. Additional details are presented in Table S9 and are given as Supporting Information in a CIF file.

Purple plates of complex **3** were grown from a tetrahydrofuran/pentane solution at 22 deg. C. A crystal of dimensions $0.31 \times 0.14 \times 0.02$ mm was mounted on a Bruker SMART APEX-I CCD-based X-ray diffractometer equipped with a low temperature device and fine focus Mo-target X-ray tube ($\lambda = 0.71073$ Å) operated at 1500 W power (50 kV, 30 mA). The X-ray intensities were measured at $85(1)$ K; the detector was placed at a distance of 5.070 cm from the crystal. A total of 2410 frames were collected with a scan width of 0.5° in ω and 0.45° in phi with an exposure time of 30 s/frame. The integration of the data yielded a total of 58,299 reflections to a maximum 2θ value of 56.62° of which 7563 were independent and 5739 were greater than $2\sigma(I)$. The final cell constants (Table S16) are based on the xyz centroids of 9982 reflections above $10\sigma(I)$. Analysis of the data showed negligible decay during data collection; the data were processed with SADABS and corrected for absorption. The structure was solved and refined with the Bruker SHELXTL (version 2018/3) software package, using the space group C2/c with Z = 4 for the formula $C_{28}H_{34}N_4O_5F_3SFe$. All non-hydrogen atoms were refined anisotropically with the hydrogen atoms placed in idealized positions. Full matrix least-squares refinement based on F2 converged at R1 = 0.0402 and wR2 = 0.0928 [based on $I > 2\sigma(I)$], R1 = 0.0623 and wR2 = 0.1052 for all data. The bound $CF_3SO_3^-$ ligand is disordered and was refined with partial occupancy orientations constrained to sum to one. Additional details are presented in Table S16 and are given as Supporting Information in a CIF file.

DFT calculations. Gaussian 09 was used to carry out all of the calculations performed here.⁴ The optimization of the structure of complex **2**, $[Fe_2(TPA)_2(NO)_2](OTf)_2$, was performed with the gradient corrected functional BP86, which has been shown to give good geometric structures for related $\{MNO\}^n$ species, and the TZVP basis set.^{5,6} Frequency calculations were further performed on the optimized structure to determine the N-O stretching frequencies.

Synthesis:

The ligand **TPA** was synthesized according to reported procedures and purity was confirmed by NMR spectroscopy.⁷ 1H -NMR (400 MHz, $CDCl_3$): δ 8.52 (ddd, 3H), 7.64 (td, 3H), 7.58 (s, 2H), 7.56 (s, 1H), 7.13 (ddd, 3H), 3.87 (s, 6H).

The ligand **BMPA-tBu₂PhOH** was synthesized according to reported procedures and purity was confirmed by NMR spectroscopy.⁸

[Fe(TPA)(CH₃CN)₂](OTf)₂: Under an inert atmosphere, 498 mg (1.15 mmol) $Fe(OTf)_2 \cdot 2CH_3CN$ and 351 mg (1.21 mmol) TPA were combined in 8 mL of CH_3CN . The reaction was stirred for 2 hours, at which point 80 mL of diethyl ether was added, causing a red solid to precipitate. Filtration gave the title compound as a red solid. Yield: 789 mg, 95%. The 1H -NMR and UV-Visible spectra of this complex are in accordance with previous literature reports.⁹

[Fe(TPA)(NO)(OTf)](OTf) (1): Under an inert atmosphere, 200 mg (0.28 mmol) of $[Fe(TPA)(CH_3CN)_2](OTf)_2$ was dissolved in a minimal volume of CH_3CN and exposed to excess NO gas, causing the solution to change color from red to dark brown. The product was precipitated by addition of 24 mL of diethyl ether. Filtration afforded the title compound as a dark brown powder. Yield: 130 mg, 68%. Single crystals suitable for X-ray diffraction were grown by vapor diffusion of diethyl ether into a concentrated CH_3CN solution of **1** in a Schlenk tube, charged with NO gas. 1H -NMR for the perchlorate analog has been reported by our laboratory previously¹⁰ (400 MHz, CD_2Cl_2 , all peaks appear as broad singlets): δ 102.1, 72.2, 64.0, 63.0, -5.0 ppm. Characterization: Elemental anal. calcd. for $C_{20}H_{18}F_6FeN_5O_7S_2$: C, 35.62; H, 2.69; N, 10.39; found (%): C, 35.73; H, 2.73; N, 10.13.

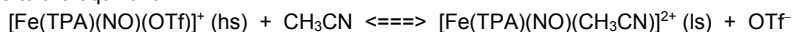
[Fe₂(TPA)₂(NO)₂](OTf)₂ (2): Under an inert atmosphere, 200 mg (0.30 mmol) of complex **1** was dissolved in a minimal volume of CH_2Cl_2 and 1 equivalent of $CoCp_2$ was added into the solution, causing the immediate color change from dark brown to orange. A minimum amount of hexane was then added to crystallize the product out overnight, which gave a crude solid mixture of **2** and a cobaltocenium impurity. The crude product was then filtered and the resulting solid was washed with a minimum amount of cold tetrahydrofuran to wash out more cobaltocenium salt. The remaining solid was dissolved in acetonitrile and a minimum amount of diethyl ether was added to recrystallize overnight. The solution was then filtered again to obtain the pure complex **2** as a black crystalline solid. 1H -NMR (700 MHz, CD_3CN): δ 10.61 (dd, 2H), 7.44 (td, 4H), 7.29 (m, 8H), 7.12 (m, 4H), 6.85 (d, 4H), 6.36 (m, 6H), 4.73 (d, 4H), 3.48 (s, 4H). Characterization: Elemental anal. calcd. for $C_{38}H_{36}F_6Fe_2N_{10}O_8S_2$: C, 43.44; H, 3.45; N, 13.33; found (%): C, 43.55; H, 3.53; N, 13.39. Mass spectrometry m/z: calcd. for the cationic half fragment $C_{18}H_{18}FeN_5O$: 376.22; Found: 376.09. Mass spectrometry m/z: calcd. for the ^{15}NO labelled cationic fragment $C_{18}H_{18}FeN_5O$: 377.09; Found: 377.09.

SUPPORTING INFORMATION

The preparation of complexes **1** and **[Fe(TPA)(NO)](BF₄)₂** (**1-BF₄**) is similar, except that Fe(BF₄)₂•2CH₃CN is used in the latter case as the iron source.

The ligand **BMPA-tBu₂PhOH**, the starting material complex **[Fe(BMPA-tBu₂PhO)(OTf)]**, and complex **3** was synthesized according to our previously reported procedure.¹¹ Single crystals of complex **3** suitable for X-ray diffraction were grown by slow diffusion of pentane into a concentrated THF solution.

Spin state changes in **1 and **1-BF₄**.** It is interesting to note that both complexes **1** and **3** have triflate bound as the sixth ligand, and even though these complexes are prepared and/or recrystallized in CH₃CN solution, the triflate remains bound in the solid state. This indicates that triflate is actually a quite strong ligand for these high-spin (hs) {FeNO}⁷ complexes. Moreover, the change in the N-O stretch between the solid and the CH₂Cl₂ solution state for these complexes is very small (1806 vs. 1800 cm⁻¹ for **1**, and 1752 vs. 1752 cm⁻¹ for **3**), again indicating that these complexes remain six-coordinate in solution with the triflate bound as the sixth ligand. In CH₃CN solution, however, complex **1** shows formation of a distinct amount of low-spin (ls) complex (by solution IR and EPR), which we attribute to the equilibrium:



where the CH₃CN-bound form is actually ls. In order to interrogate this point further, we then prepared the complex **1-BF₄** where the triflate is replaced by the much more weakly coordinating counter ion BF₄⁻. This complex is again hs in the solid state and when dissolved in CH₃CN, shows formation of a large fraction of the ls complex. In solution at room temperature, the hs state is still dominant, although it is not a priori clear whether this fraction of the complex is either five-coordinate or six-coordinate with BF₄⁻ bound. The hs N-O band in the solution IR spectrum is broad and shows at least two components (see Figure S10, top), and the exact nature of these species is not clear. Upon cooling and freezing the solution, more of the CH₃CN-bound complex forms, driven by entropy, resulting in an EPR spectrum that now almost exclusively shows the ls state. In comparison to **1**, the EPR data in CH₃CN solution therefore show quite clearly that it is indeed CH₃CN coordination that is responsible for the formation of the ls state of **1**.

SUPPORTING INFORMATION

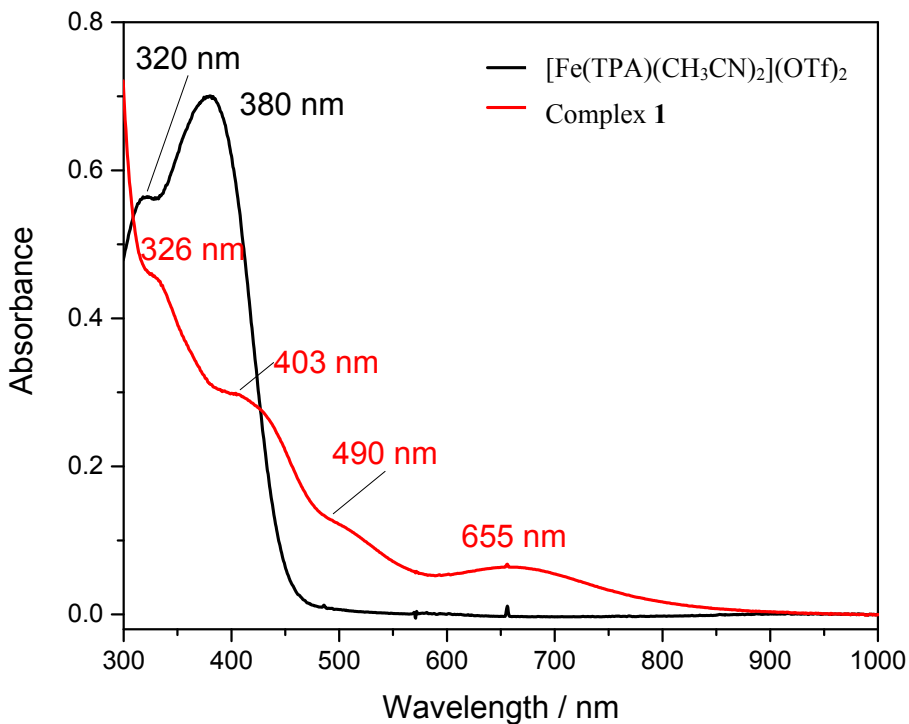


Figure S1. UV-Vis absorption spectra of complexes $[\text{Fe}(\text{TPA})(\text{CH}_3\text{CN})_2](\text{OTf})_2$ and **1** in CH_2Cl_2 at ~ 0.25 mM concentration at room temperature.

SUPPORTING INFORMATION

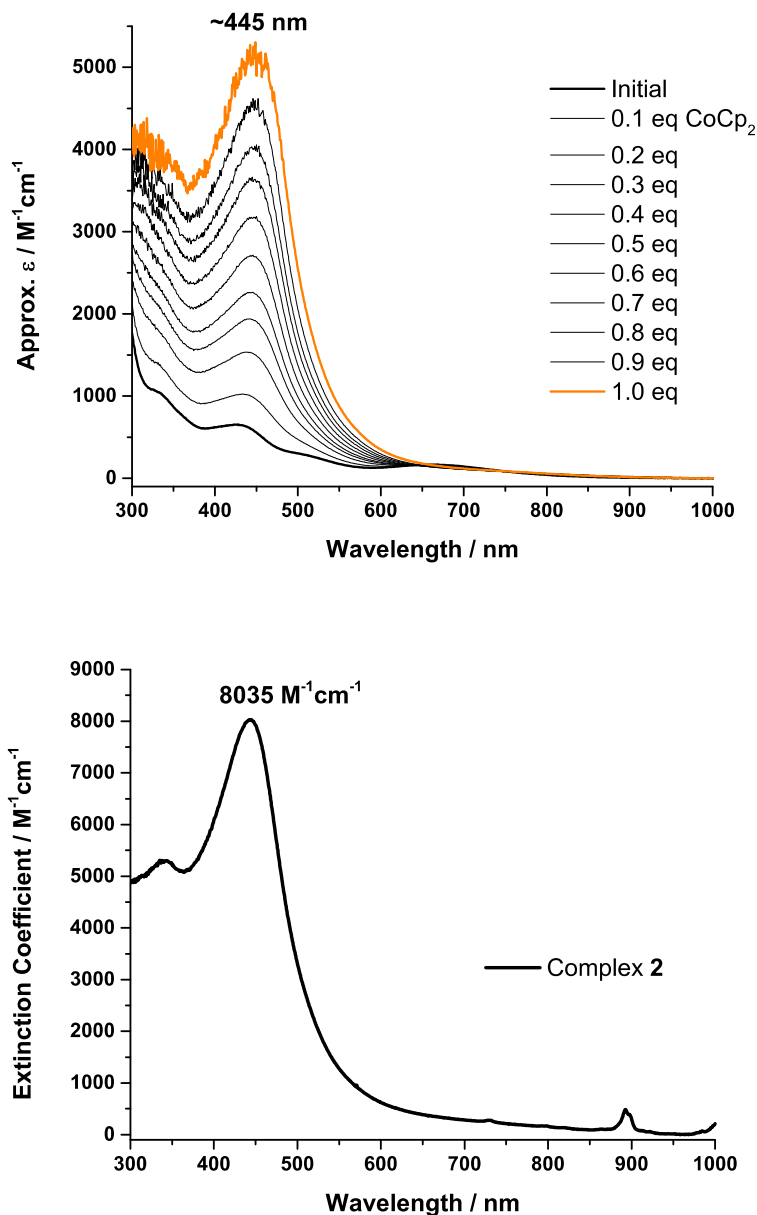


Figure S2. Top: UV-Vis dip probe titration experiment of complex **1** (initial black line) with CoCp₂, showing formation of **2** (orange line) in CH₂Cl₂ at ~0.25 mM concentration at room temperature. Only an approximate extinction coefficient is given due to the highly concentrated sample. **Bottom:** UV-Vis spectrum of a pure solution of **2** at ~0.083 mM concentration at room temperature, showing an extinction coefficient of 8035 M⁻¹cm⁻¹ at $\lambda_{\text{max}} = 445$ nm.

SUPPORTING INFORMATION

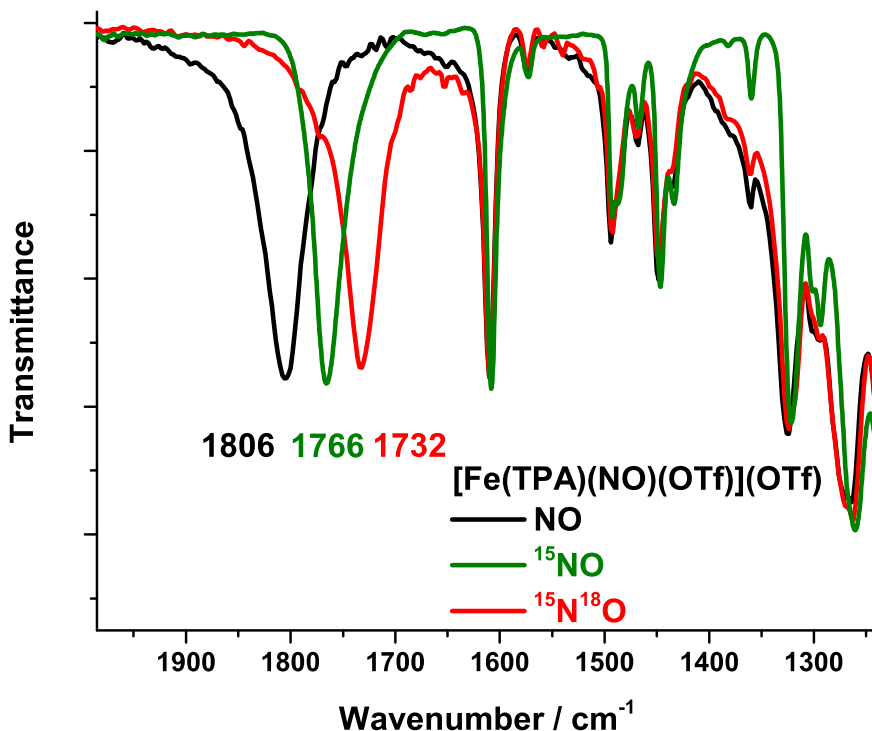


Figure S3. FT-IR spectra of complex **1** in KBr disks with natural abundance NO (black), ^{15}NO (green) and $^{15}\text{N}^{18}\text{O}$ (red), showing the N-O stretching frequency at 1806 cm^{-1} that is isotopically shifted.

SUPPORTING INFORMATION

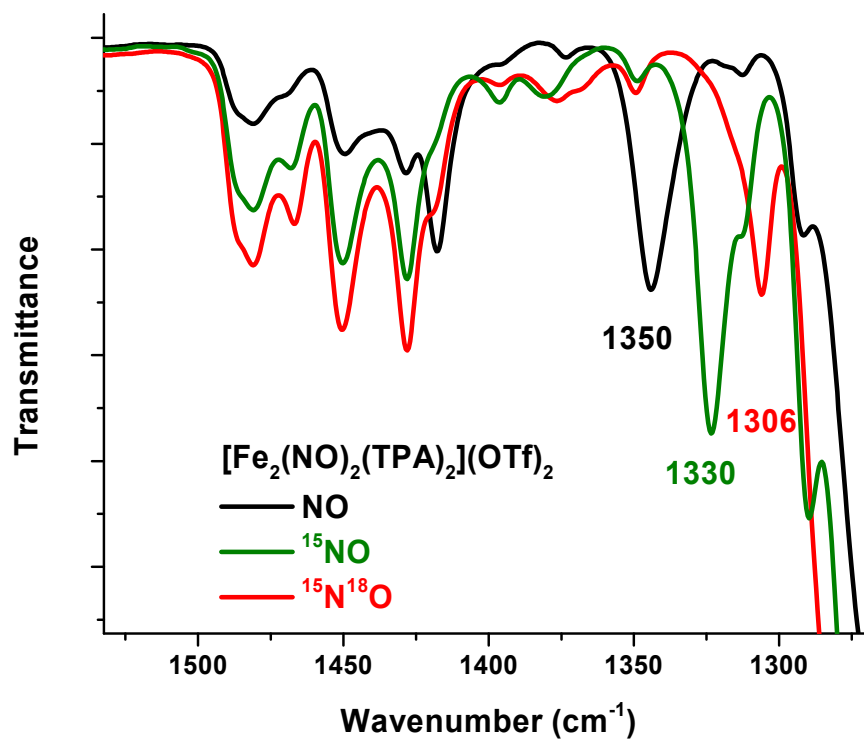


Figure S4. FT-IR spectra of complex **2** in KBr disks with natural abundance NO (black), ^{15}NO (green) and $^{15}\text{N}^{18}\text{O}$ (red), showing the antisymmetric N-O stretching frequency at 1350 cm^{-1} that is isotopically shifted.

SUPPORTING INFORMATION

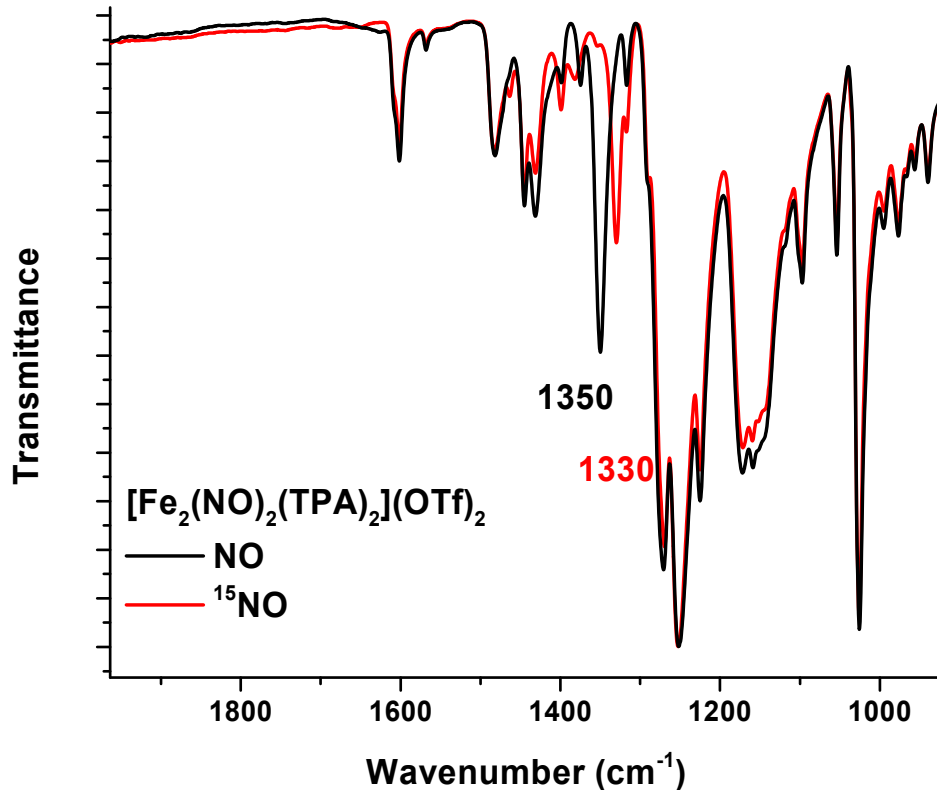


Figure S5. FT-IR spectra of complex **2** in KBr disks with natural abundance NO (black) and ¹⁵NO (red), showing complete overlap of the ligand features whereas the NO signals are isotopically shifted.

SUPPORTING INFORMATION

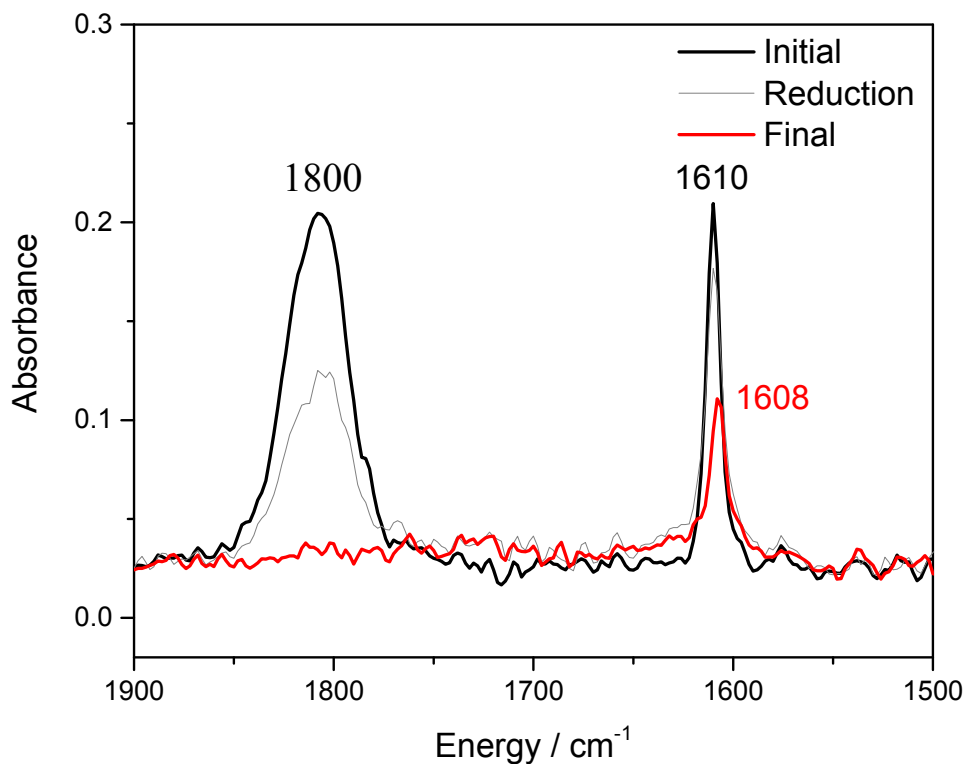


Figure S6. IR spectro-electrochemistry showing the reduction of **1** in CH_2Cl_2 with 0.1 M NBu_4PF_6 as supporting electrolyte. Upon reduction, the N-O stretch of **1** at 1800 cm^{-1} disappears, but no new signal that would correspond to a $\text{hs-}\{\text{FeNO}\}^8$ complex or a DNIC appears within the $1500\text{-}1800 \text{ cm}^{-1}$ range. Note that the sharp signal at 1610 cm^{-1} corresponds to a ligand band (see Figure S3).

SUPPORTING INFORMATION

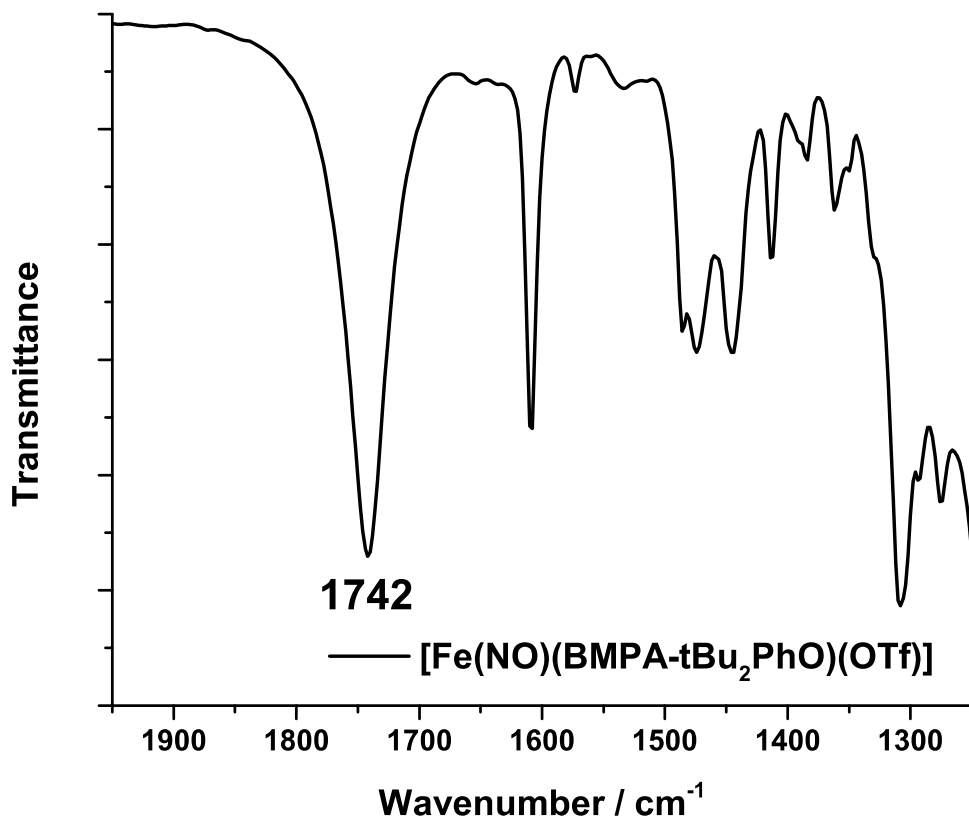


Figure S7. FT-IR spectrum of complex **3** (black) in a KBr disk showing the N-O stretching frequency at 1742 cm⁻¹.

SUPPORTING INFORMATION

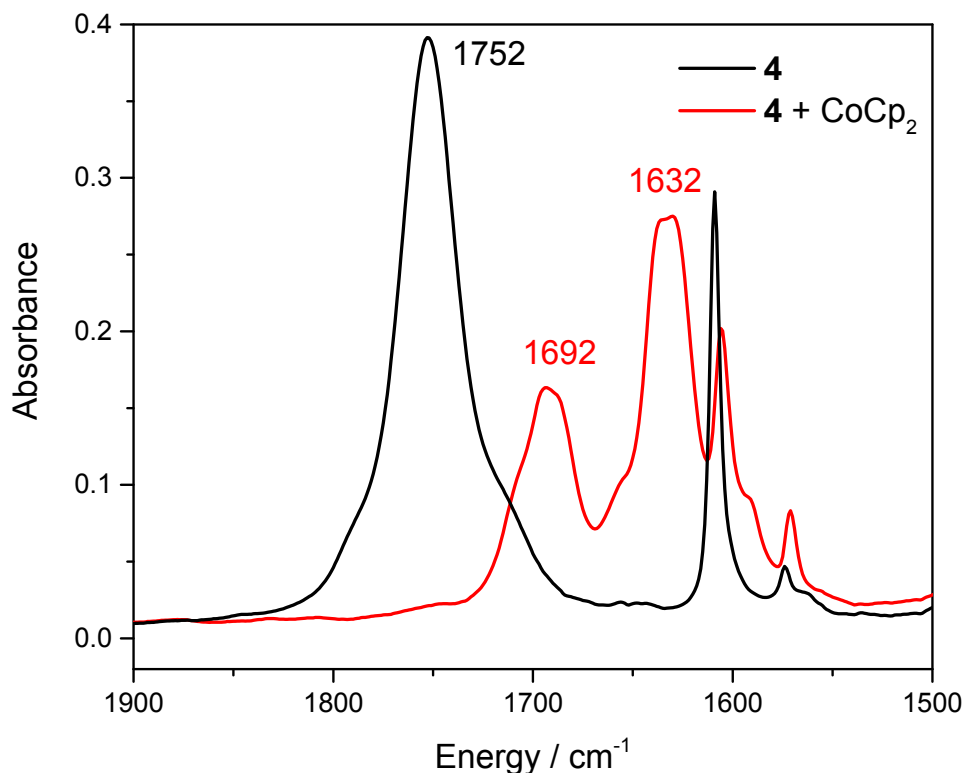


Figure S8. Solution IR spectra of **3** (black) and of **3** treated with cobaltocene (red), showing the formation of the DNIC product. Spectra were recorded in CH_2Cl_2 at room temperature.

SUPPORTING INFORMATION

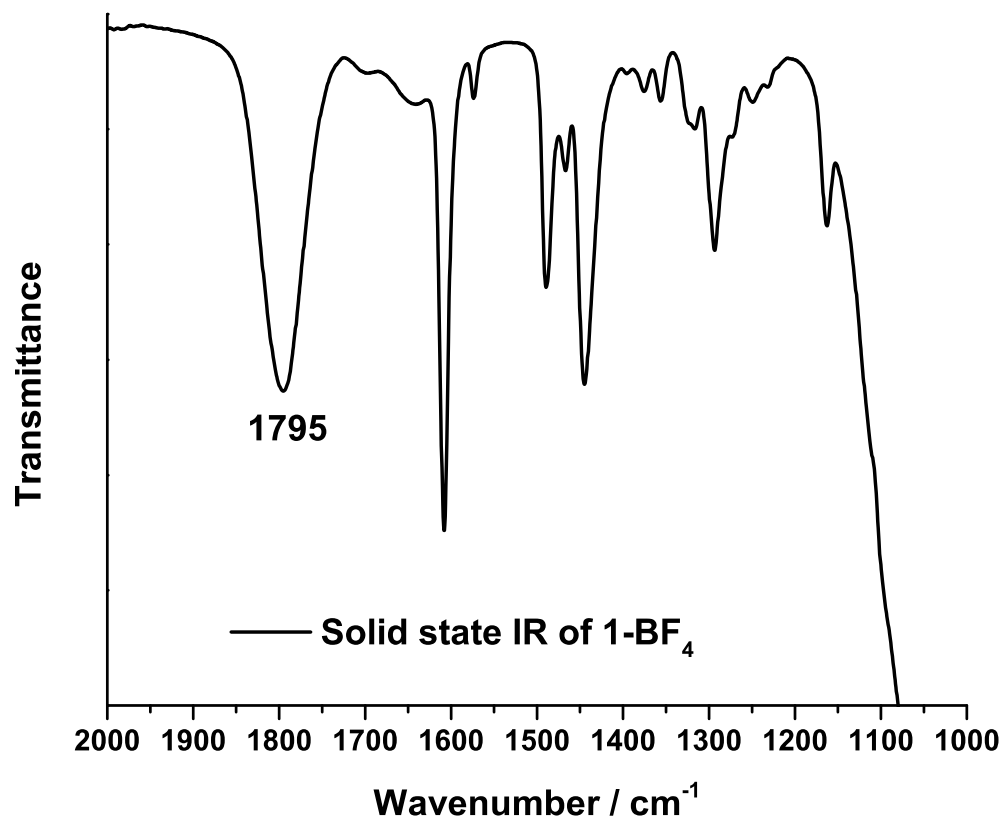


Figure S9. FT-IR spectrum of complex **1**-BF₄ (black) in the solid state, showing the N-O stretching frequency at 1795 cm⁻¹.

SUPPORTING INFORMATION

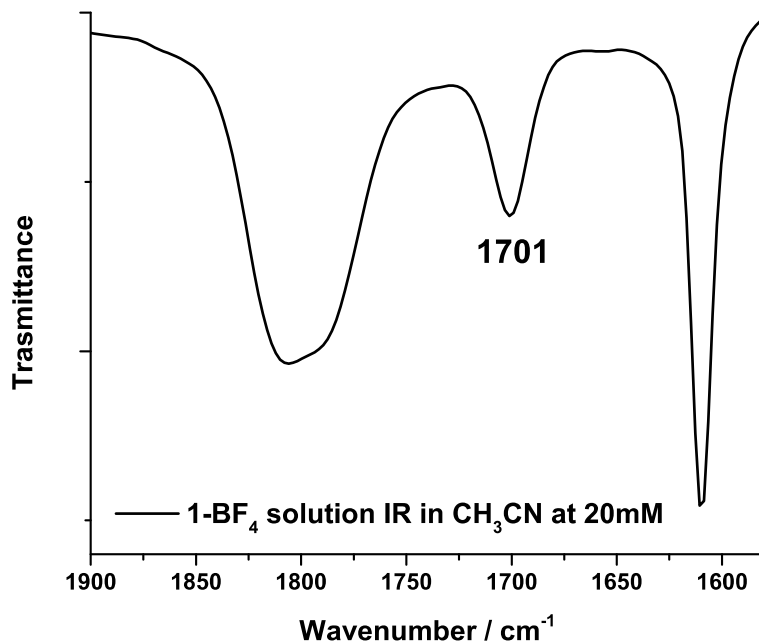


Figure S10. FT-IR spectrum of 20 mM complex **1-BF₄** (black) in CH₃CN solution at room temperature, showing the N-O stretching frequency of the ls component at 1701 cm^{-1} .

SUPPORTING INFORMATION

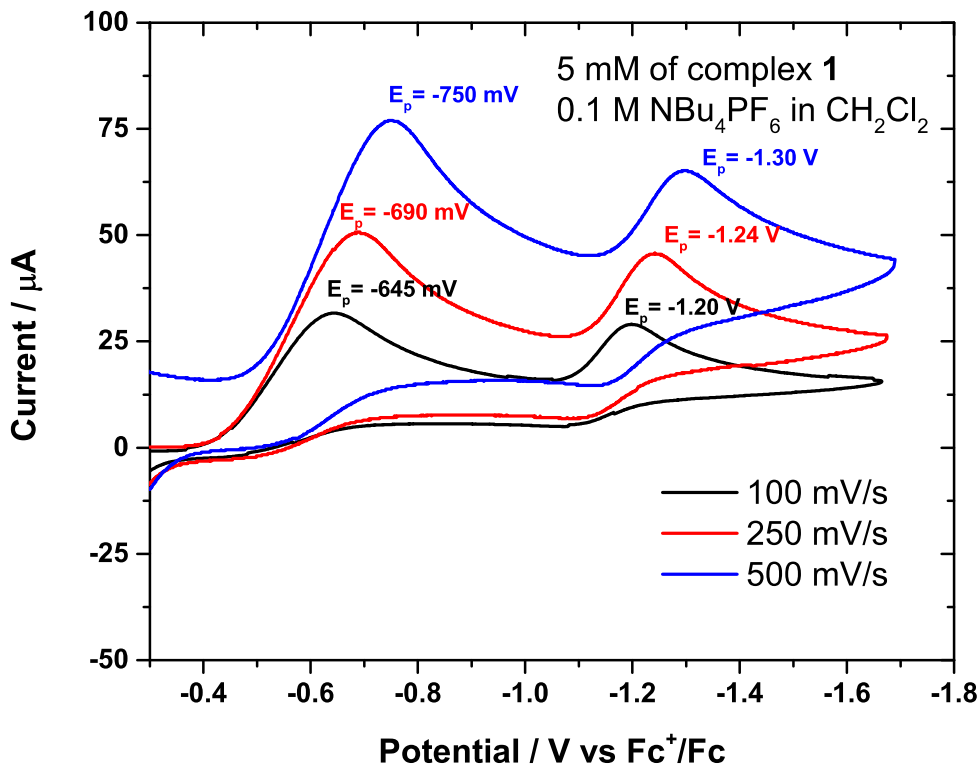


Figure S11. Cyclic voltammogram of a 5 mM solution of complex **1** in CH_2Cl_2 containing 0.1 M $[\text{NBu}_4]\text{PF}_6$ as supporting electrolyte. The signals are referenced against Fc^+/Fc and the scan rate is varied as indicated. A three-component cell was used consisting of a glassy carbon working electrode, a platinum auxiliary electrode, and a Ag wire pseudoreference electrode.

SUPPORTING INFORMATION

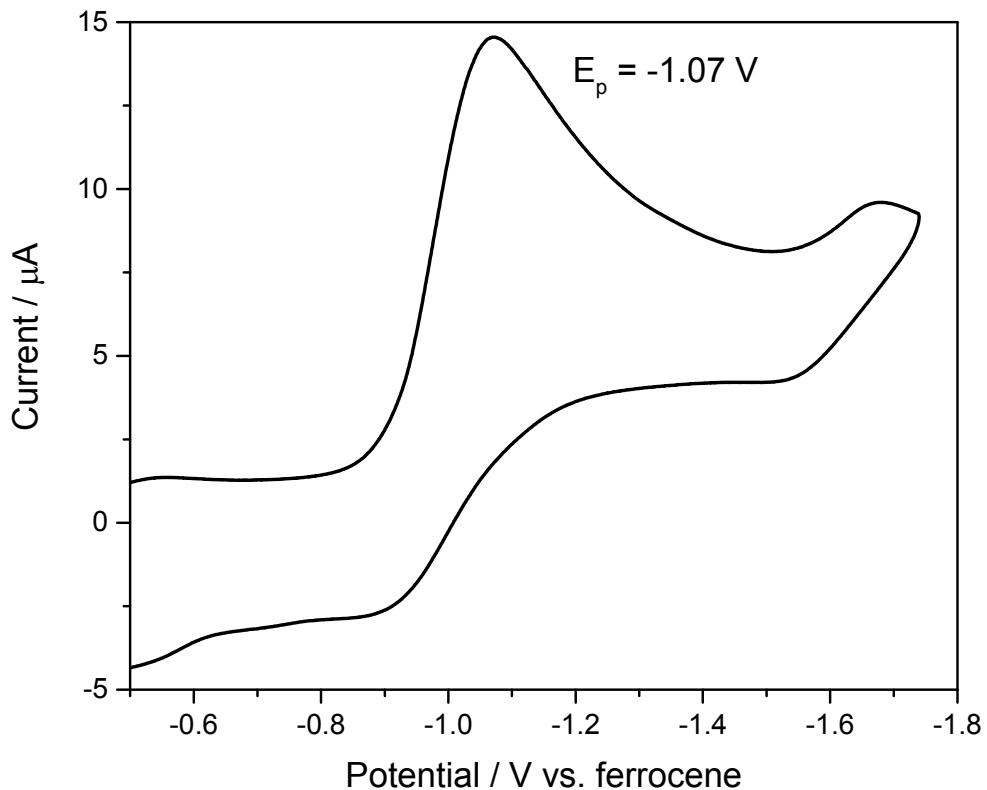


Figure S12. Cyclic voltammogram of 5 mM complex **3** in CH_2Cl_2 containing 0.1 M $[\text{NBu}_4](\text{ClO}_4)$ as supporting electrolyte. Scan rate: 200 mV/s. The signals are referenced against Fc^+/Fc . A three-component cell was used consisting of a glassy carbon working electrode, a platinum auxiliary electrode, and a Ag wire pseudoreference electrode.

SUPPORTING INFORMATION

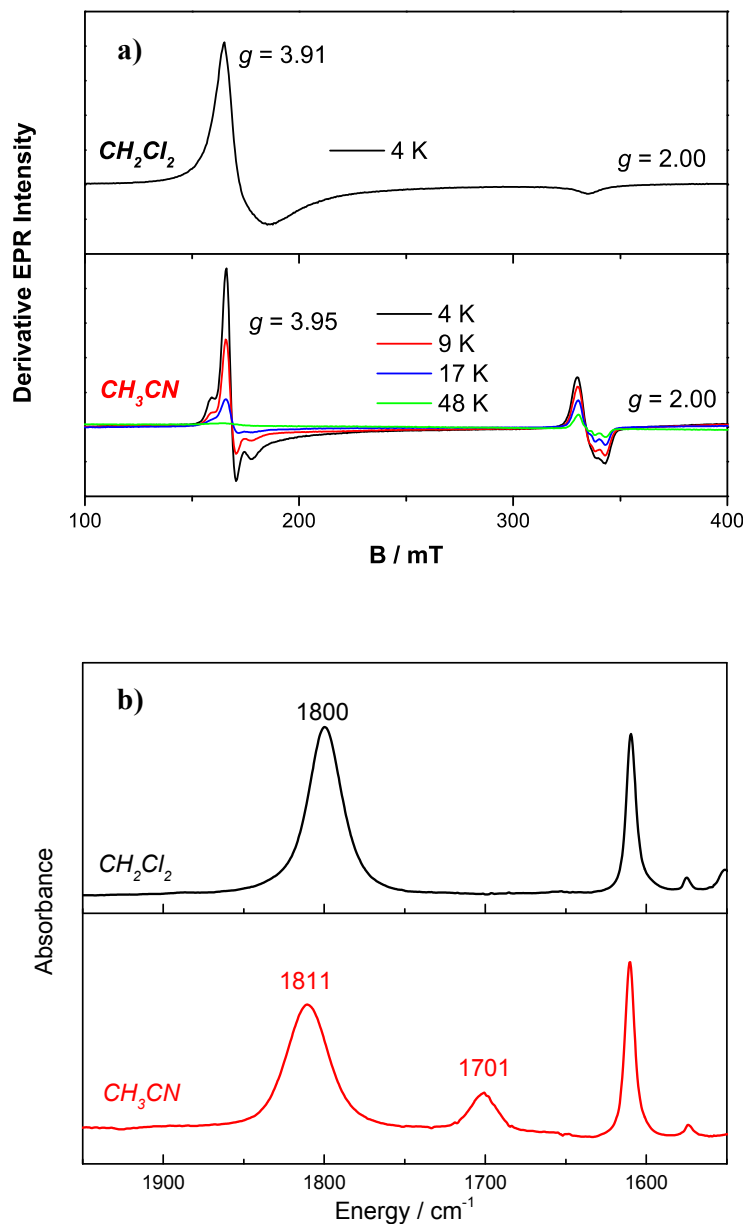


Figure S13. **Panel a)** EPR spectrum of **1** in CH_2Cl_2 at 4 K showing 100% of the hs- $\{\text{FeNO}\}^7$ complex with $S_t = 3/2$ (top) vs. the EPR spectrum of **1** in CH_3CN at various temperatures, where a noticeable portion of the compound is converted to a ls- $\{\text{FeNO}\}^7$ complex with $S_t = 1/2$. **Panel b)** Solution IR spectrum of **1** in CH_2Cl_2 at room temperature, showing the N-O stretch at 1800 cm^{-1} , which belongs to the hs- $\{\text{FeNO}\}^7$ complex (top) vs. the solution IR spectrum of **1** in CH_3CN at room temperature, showing conversion of a fraction of **1** to a ls complex with the N-O stretch at 1701 cm^{-1} .

SUPPORTING INFORMATION

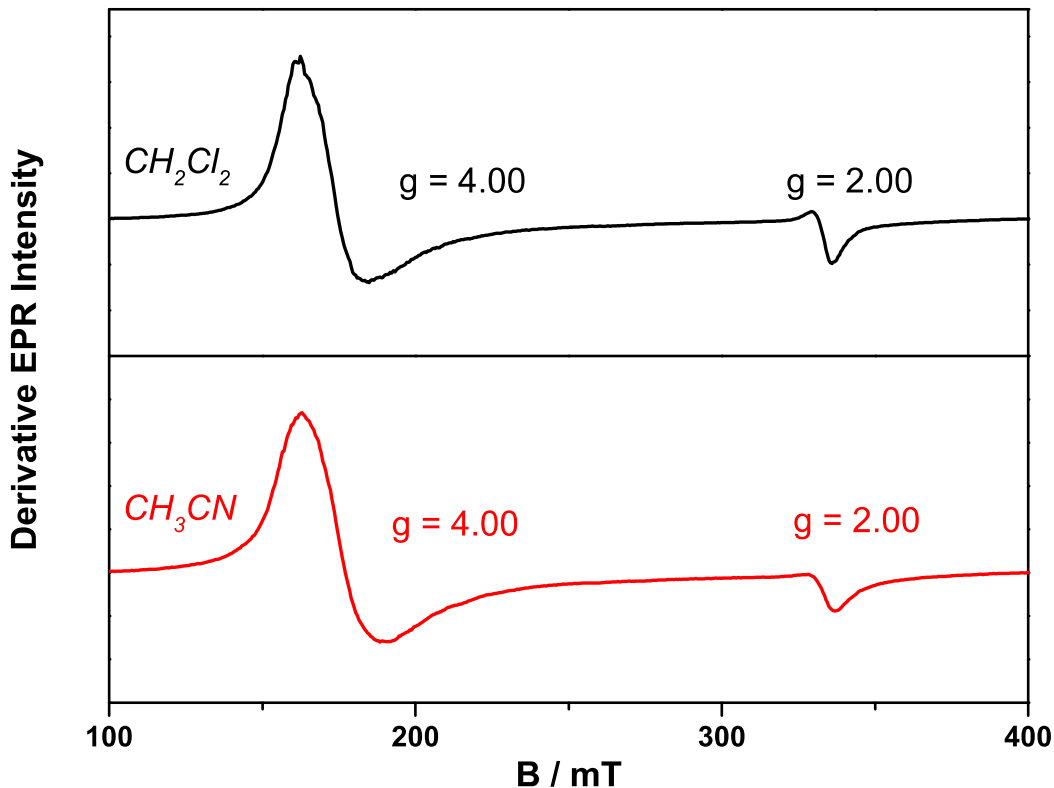


Figure S14. EPR spectrum of **3** at 4 K in CH_2Cl_2 (top) and CH_3CN (bottom), showing 100% of the hs- $\{\text{FeNO}\}^7$ complex with $S_t = 3/2$.

SUPPORTING INFORMATION

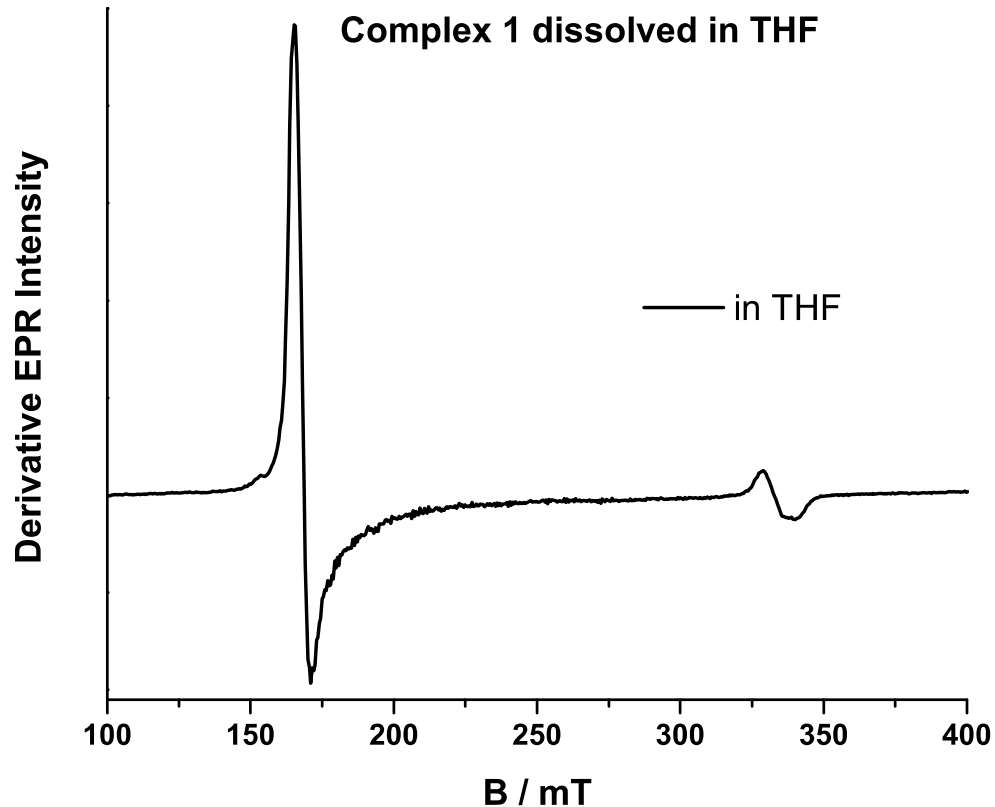


Figure S15. EPR spectrum of **1** in tetrahydrofuran at 4 K and 2 mM concentration, showing exclusively the presence of the hs- $\{\text{FeNO}\}^7$ complex with $S_t = 3/2$.

SUPPORTING INFORMATION

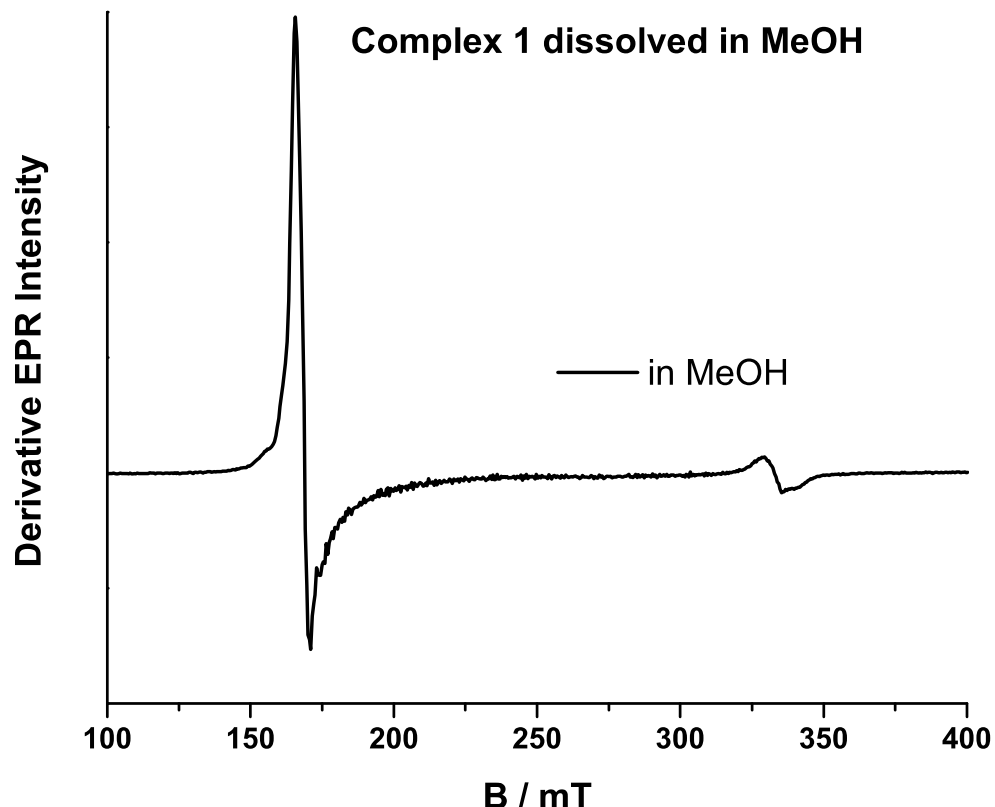


Figure S16. EPR spectrum of **1** in methanol at 4 K and 2 mM concentration, showing exclusively the presence of the hs- $\{\text{FeNO}\}^7$ complex with $S_{\text{t}} = 3/2$.

SUPPORTING INFORMATION

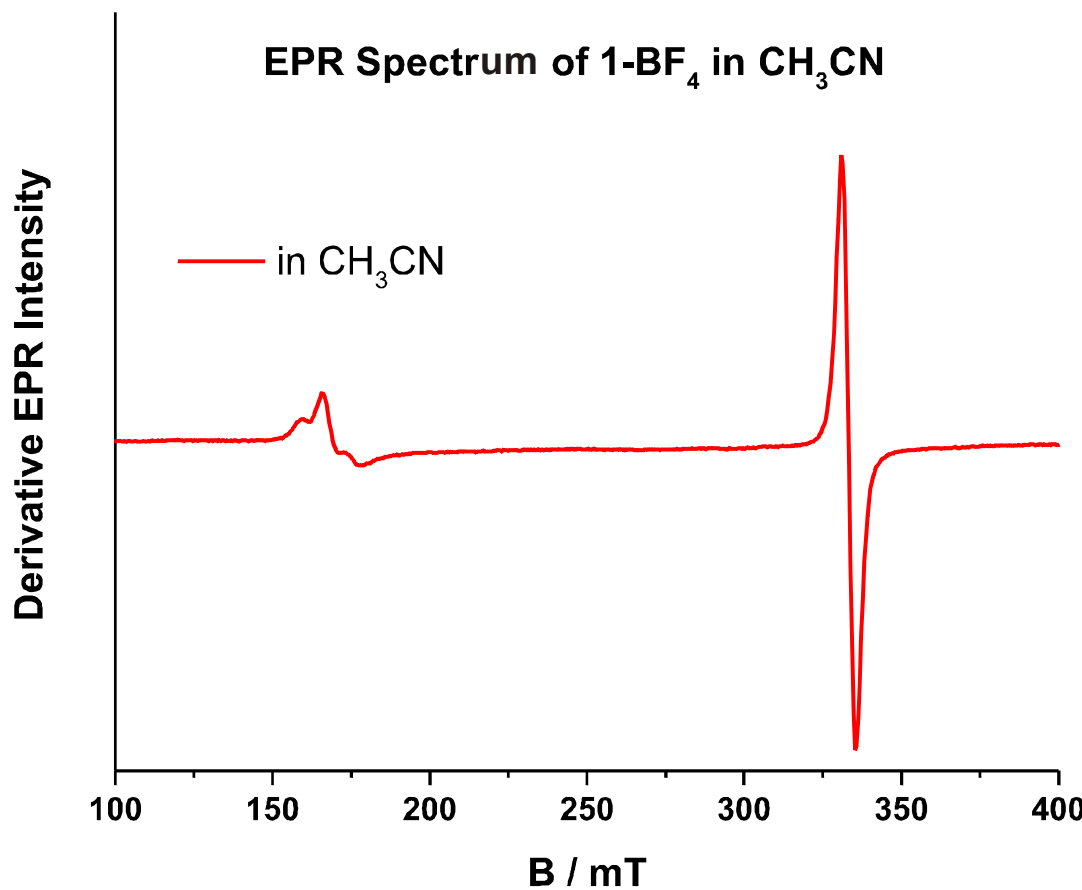


Figure S17. EPR spectrum of $\mathbf{1}\text{-BF}_4$ at 4 K and 2 mM in CH_3CN , showing predominant formation of a ls- $\{\text{FeNO}\}^7$ complex with $S_t = 1/2$.

SUPPORTING INFORMATION

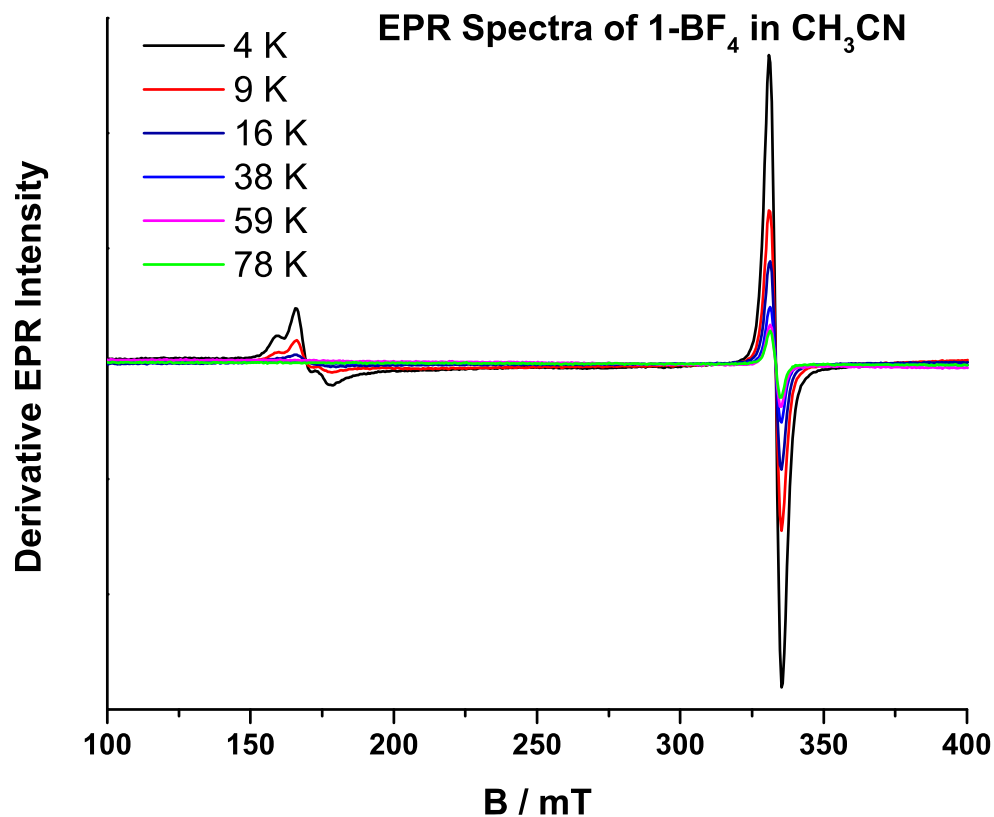


Figure S18. EPR spectra of $\mathbf{1}\text{-BF}_4$ in CH_3CN at the indicated temperatures and 2 mM concentration, showing almost exclusive formation of a $\text{1s-}\{\text{FeNO}\}^7$ complex with $S_t = 1/2$.

SUPPORTING INFORMATION

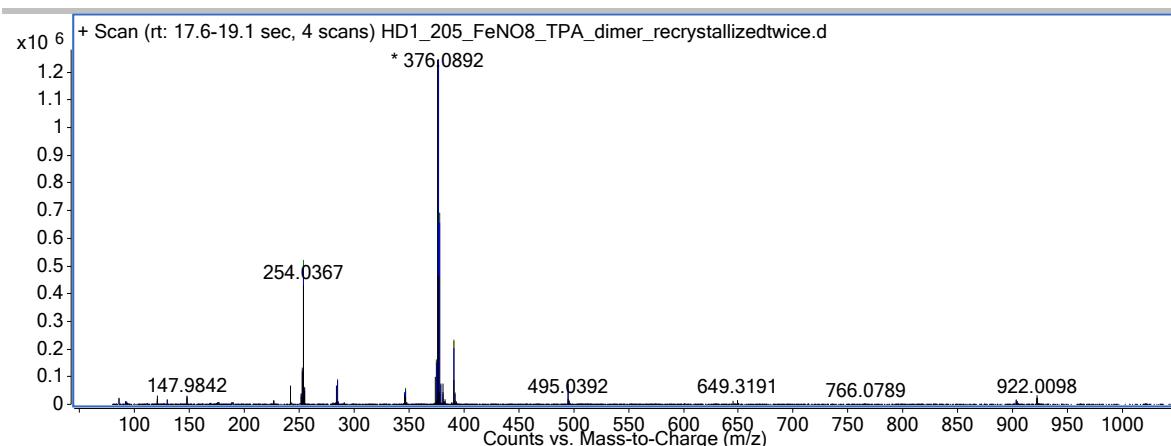


Figure S19. Mass spectrometry showing the m/z fragment of complex **2** with natural abundance isotopes NO ($m/z = 376.09$).

SUPPORTING INFORMATION

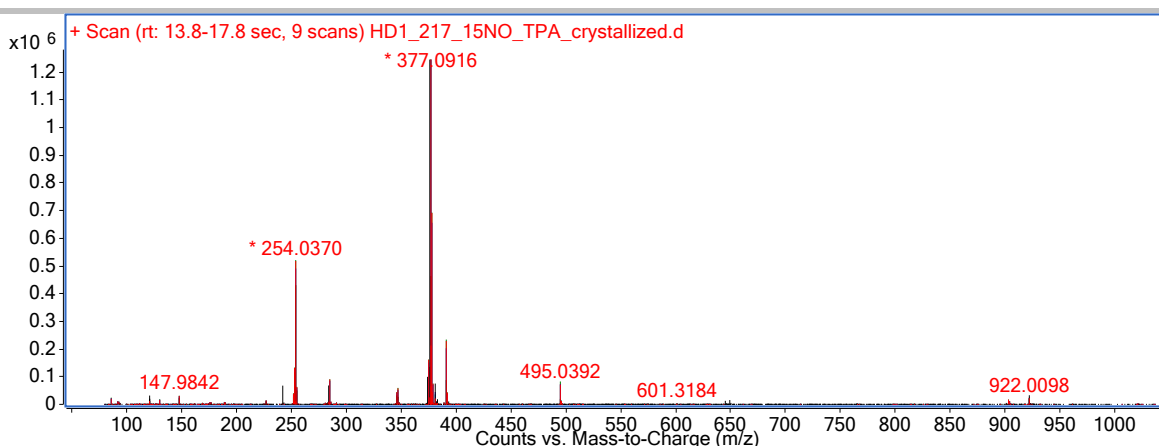


Figure S20. Mass spectrometry showing the m/z fragment of complex **2** with ^{15}NO ($m/z = 377.09$).

SUPPORTING INFORMATION

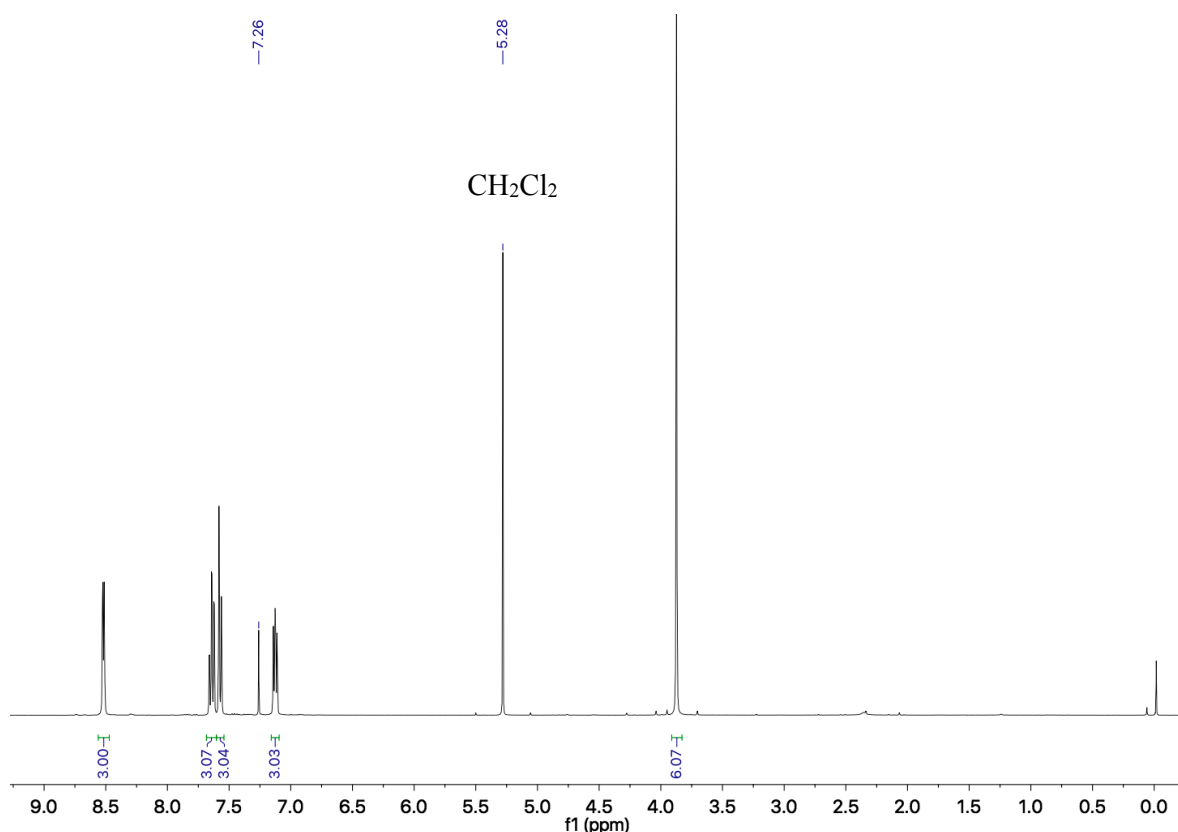


Figure S21. ¹H-NMR spectrum of the TPA ligand, measured in CDCl₃ at room temperature. Residual CH₂Cl₂ shows a peak at 5.28 ppm.

SUPPORTING INFORMATION

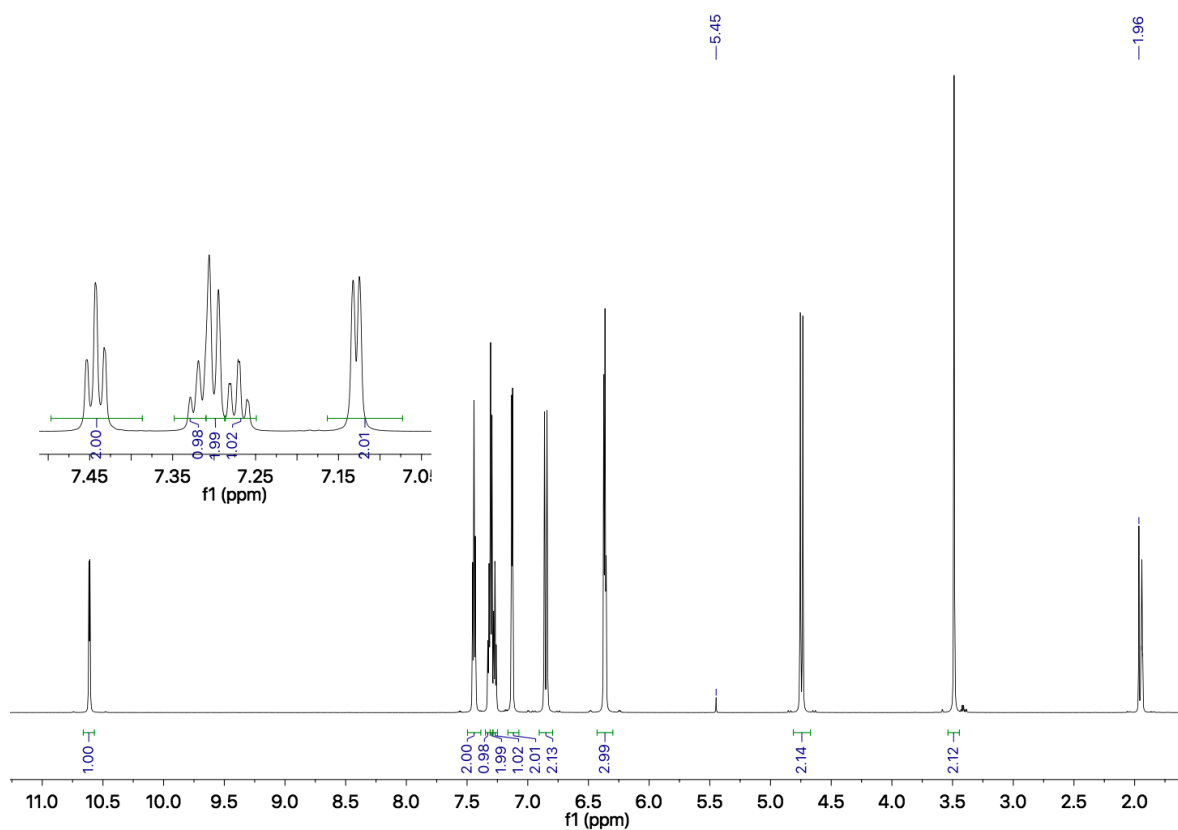


Figure S22. ¹H-NMR spectrum of complex 2 in CD₃CN, showing a completely diamagnetic NMR spectrum, supporting the $S_t = 0$ assignment of 2, which is further confirmed by the Evans method. The spectrum is referenced against solvent residual signal.

SUPPORTING INFORMATION

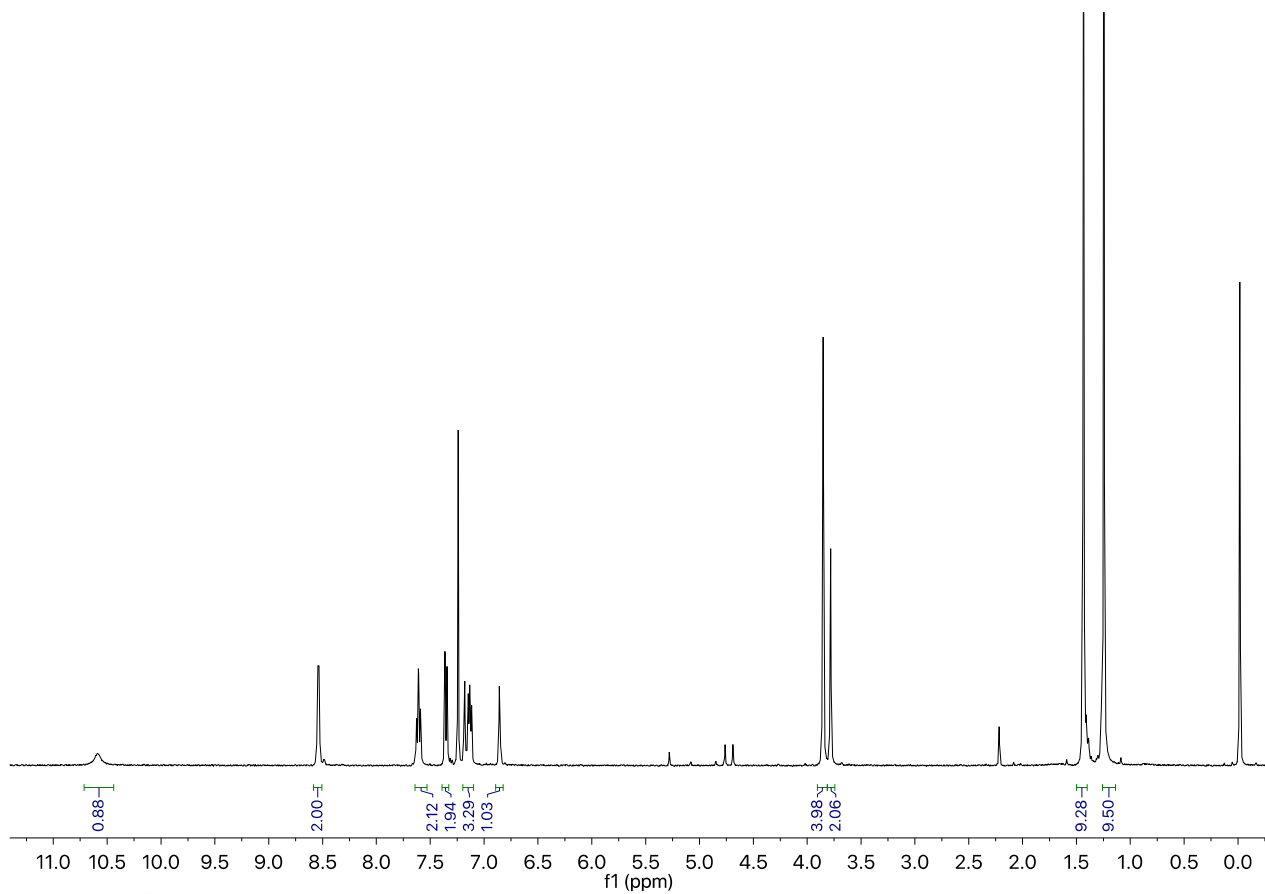


Figure S23. ¹H-NMR spectrum of the BMPA-tBu₂PhOH ligand, measured in CDCl₃ at room temperature.

SUPPORTING INFORMATION

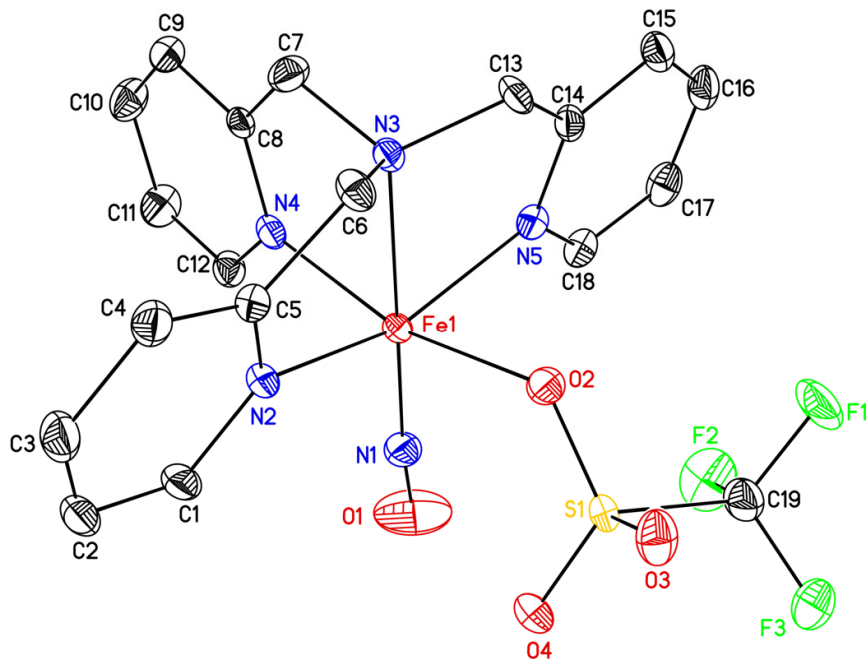


Figure S24. Crystal structure of complex **1** with ellipsoids drawn at 50% probability. The triflate counter anion, solvent molecules, and hydrogen atoms are omitted for clarity. The atomic labelling scheme is indicated.

Table S1. Important crystal parameters of complex **1**.

Selected bonds/angles	Å/deg.
Fe1–N1	1.755
N1–O1	1.144
Fe1–N2	2.138
Fe1–N3	2.218
Fe1–N4	2.109
Fe1–N5	2.135
F1–O2	2.148
Fe1–N1–O1	170

SUPPORTING INFORMATION**Table S2.** Crystal data and structure refinement for complex **1**.

Identification code	als4240
Empirical formula	C ₂₀ H ₁₈ F ₆ FeN ₅ O ₇ S ₂
Formula weight	674.36
Temperature	85(2) K
Wavelength	1.54178 Å
Crystal system, space group	Triclinic, P-1
Unit cell dimensions	a = 8.8570(2) Å alpha = 86.680(6) deg. b = 9.1861(2) Å beta = 86.645(6) deg. c = 17.2751(12) Å gamma = 68.350(5) deg.
Volume	1303.13(11) Å ³
Z, Calculated density	2, 1.719 Mg/m ³
Absorption coefficient	7.019 mm ⁻¹
F(000)	682
Crystal size	0.200 x 0.140 x 0.080 mm
Theta range for data collection	2.564 to 68.238 deg.
Limiting indices	-10<=h<=10, -11<=k<=11, -20<=l<=20
Reflections collected / unique	35038 / 4698 [R(int) = 0.0563]
Completeness to theta = 67.679	98.8 %
Absorption correction	Semi-empirical from equivalents
Max. and min. transmission	0.568 and 0.307
Refinement method	Full-matrix least-squares on F ²
Data / restraints / parameters	4698 / 0 / 370
Goodness-of-fit on F ²	1.089
Final R indices [I>2σ(I)]	R1 = 0.0311, wR2 = 0.0843
R indices (all data)	R1 = 0.0315, wR2 = 0.0846
Extinction coefficient	n/a
Largest diff. peak and hole	0.290 and -0.578 e.Å ⁻³

SUPPORTING INFORMATION

Table S3. Atomic coordinates ($\times 10^4$) and equivalent isotropic displacement parameters ($\text{\AA}^2 \times 10^3$) for complex **1**.
U(eq) is defined as one third of the trace of the orthogonalized Uij tensor.

	x	y	z	U(eq)
Fe(1)	4092(1)	6702(1)	7369(1)	13(1)
S(1)	2210(1)	5991(1)	5915(1)	14(1)
S(2)	10516(1)	2264(1)	8692(1)	18(1)
F(1)	2096(2)	8238(2)	4887(1)	35(1)
F(2)	627(2)	9023(2)	5934(1)	39(1)
F(3)	-155(2)	7864(2)	5080(1)	33(1)
F(4)	9095(2)	2446(2)	10078(1)	36(1)
F(5)	7434(2)	3434(2)	9152(1)	28(1)
F(6)	8555(2)	929(2)	9325(1)	32(1)
N(1)	2079(2)	7379(2)	7745(1)	20(1)
N(2)	4950(2)	4224(2)	7597(1)	16(1)
N(3)	6653(2)	5919(2)	6921(1)	13(1)
N(4)	5210(2)	7071(2)	8345(1)	15(1)
N(5)	4213(2)	8804(2)	6824(1)	15(1)
O(1)	787(2)	8030(3)	7986(1)	51(1)
O(2)	3594(2)	6246(2)	6224(1)	17(1)
O(3)	2672(2)	4912(2)	5303(1)	23(1)
O(4)	1057(2)	5823(2)	6497(1)	23(1)
O(5)	11831(2)	884(2)	8954(1)	26(1)
O(6)	10672(2)	3731(2)	8831(1)	24(1)
O(7)	9964(2)	2172(2)	7934(1)	26(1)
C(1)	4205(3)	3468(3)	8084(1)	21(1)
C(2)	4862(3)	1862(3)	8223(1)	25(1)
C(3)	6324(3)	1014(2)	7857(1)	25(1)
C(4)	7092(3)	1778(2)	7352(1)	20(1)
C(5)	6364(2)	3386(2)	7236(1)	16(1)
C(6)	7088(2)	4292(2)	6670(1)	16(1)
C(7)	7717(2)	5953(2)	7553(1)	19(1)
C(8)	6825(2)	6712(2)	8277(1)	13(1)
C(9)	7673(3)	6985(2)	8869(1)	18(1)
C(10)	6841(3)	7639(3)	9542(1)	25(1)
C(11)	5171(3)	8010(3)	9607(1)	24(1)
C(12)	4404(3)	7706(2)	9001(1)	18(1)
C(13)	6722(2)	6982(2)	6252(1)	16(1)
C(14)	5536(2)	8624(2)	6359(1)	15(1)
C(15)	5735(3)	9893(2)	5946(1)	19(1)
C(16)	4530(3)	11363(2)	6005(1)	22(1)
C(17)	3170(3)	11550(2)	6482(1)	22(1)
C(18)	3057(3)	10244(2)	6890(1)	18(1)
C(19)	1136(3)	7878(2)	5429(1)	23(1)
C(20)	8809(3)	2270(3)	9346(1)	23(1)

SUPPORTING INFORMATION

Table S4. Bond lengths [Å] and angles [deg] for complex **1**.

Fe(1)-N(1)	1.7548(18)
Fe(1)-N(4)	2.1086(16)
Fe(1)-N(5)	2.1351(16)
Fe(1)-N(2)	2.1378(17)
Fe(1)-O(2)	2.1484(13)
Fe(1)-N(3)	2.2178(16)
S(1)-O(3)	1.4285(14)
S(1)-O(4)	1.4324(14)
S(1)-O(2)	1.4646(14)
S(1)-C(19)	1.823(2)
S(2)-O(6)	1.4388(15)
S(2)-O(5)	1.4409(15)
S(2)-O(7)	1.4430(14)
S(2)-C(20)	1.832(2)
F(1)-C(19)	1.336(2)
F(2)-C(19)	1.334(3)
F(3)-C(19)	1.327(3)
F(4)-C(20)	1.335(2)
F(5)-C(20)	1.336(3)
F(6)-C(20)	1.334(2)
N(1)-O(1)	1.144(3)
N(2)-C(5)	1.343(3)
N(2)-C(1)	1.352(2)
N(3)-C(13)	1.483(2)
N(3)-C(6)	1.483(2)
N(3)-C(7)	1.492(2)
N(4)-C(8)	1.344(3)
N(4)-C(12)	1.345(3)
N(5)-C(14)	1.344(3)
N(5)-C(18)	1.348(3)
C(1)-C(2)	1.384(3)
C(1)-H(1)	0.9500
C(2)-C(3)	1.378(3)
C(2)-H(2)	0.9500
C(3)-C(4)	1.389(3)
C(3)-H(3)	0.9500
C(4)-C(5)	1.384(3)
C(4)-H(4)	0.9500
C(5)-C(6)	1.513(2)
C(6)-H(6A)	0.9900
C(6)-H(6B)	0.9900
C(7)-C(8)	1.501(3)
C(7)-H(7A)	0.9900
C(7)-H(7B)	0.9900
C(8)-C(9)	1.390(3)
C(9)-C(10)	1.382(3)
C(9)-H(9)	0.9500

SUPPORTING INFORMATION

C(10)-C(11)	1.389(3)
C(10)-H(10)	0.9500
C(11)-C(12)	1.377(3)
C(11)-H(11)	0.9500
C(12)-H(12)	0.9500
C(13)-C(14)	1.502(3)
C(13)-H(13A)	0.9900
C(13)-H(13B)	0.9900
C(14)-C(15)	1.392(3)
C(15)-C(16)	1.383(3)
C(15)-H(15)	0.9500
C(16)-C(17)	1.382(3)
C(16)-H(16)	0.9500
C(17)-C(18)	1.388(3)
C(17)-H(17)	0.9500
C(18)-H(18)	0.9500
N(1)-Fe(1)-N(4)	98.06(7)
N(1)-Fe(1)-N(5)	100.87(7)
N(4)-Fe(1)-N(5)	89.77(6)
N(1)-Fe(1)-N(2)	104.31(7)
N(4)-Fe(1)-N(2)	92.63(6)
N(5)-Fe(1)-N(2)	154.09(7)
N(1)-Fe(1)-O(2)	97.36(7)
N(4)-Fe(1)-O(2)	164.18(6)
N(5)-Fe(1)-O(2)	83.86(5)
N(2)-Fe(1)-O(2)	86.97(6)
N(1)-Fe(1)-N(3)	177.66(7)
N(4)-Fe(1)-N(3)	80.01(6)
N(5)-Fe(1)-N(3)	77.86(6)
N(2)-Fe(1)-N(3)	77.17(6)
O(2)-Fe(1)-N(3)	84.49(5)
O(3)-S(1)-O(4)	117.29(9)
O(3)-S(1)-O(2)	112.92(9)
O(4)-S(1)-O(2)	114.23(8)
O(3)-S(1)-C(19)	103.95(9)
O(4)-S(1)-C(19)	104.12(10)
O(2)-S(1)-C(19)	101.97(9)
O(6)-S(2)-O(5)	115.31(9)
O(6)-S(2)-O(7)	114.62(9)
O(5)-S(2)-O(7)	114.77(9)
O(6)-S(2)-C(20)	103.32(9)
O(5)-S(2)-C(20)	102.99(9)
O(7)-S(2)-C(20)	103.49(9)
O(1)-N(1)-Fe(1)	170.05(17)
C(5)-N(2)-C(1)	118.88(17)
C(5)-N(2)-Fe(1)	115.94(12)
C(1)-N(2)-Fe(1)	125.16(15)
C(13)-N(3)-C(6)	110.81(14)
C(13)-N(3)-C(7)	112.11(14)
C(6)-N(3)-C(7)	110.28(15)
C(13)-N(3)-Fe(1)	107.37(12)
C(6)-N(3)-Fe(1)	106.65(11)
C(7)-N(3)-Fe(1)	109.42(11)
C(8)-N(4)-C(12)	119.05(16)
C(8)-N(4)-Fe(1)	116.51(12)
C(12)-N(4)-Fe(1)	124.35(13)

SUPPORTING INFORMATION

C(14)-N(5)-C(18)	119.13(16)
C(14)-N(5)-Fe(1)	115.64(12)
C(18)-N(5)-Fe(1)	125.17(13)
S(1)-O(2)-Fe(1)	132.26(8)
N(2)-C(1)-C(2)	121.9(2)
N(2)-C(1)-H(1)	119.0
C(2)-C(1)-H(1)	119.0
C(3)-C(2)-C(1)	118.82(19)
C(3)-C(2)-H(2)	120.6
C(1)-C(2)-H(2)	120.6
C(2)-C(3)-C(4)	119.68(19)
C(2)-C(3)-H(3)	120.2
C(4)-C(3)-H(3)	120.2
C(5)-C(4)-C(3)	118.5(2)
C(5)-C(4)-H(4)	120.7
C(3)-C(4)-H(4)	120.7
N(2)-C(5)-C(4)	122.17(18)
N(2)-C(5)-C(6)	116.12(16)
C(4)-C(5)-C(6)	121.67(18)
N(3)-C(6)-C(5)	110.39(15)
N(3)-C(6)-H(6A)	109.6
C(5)-C(6)-H(6A)	109.6
N(3)-C(6)-H(6B)	109.6
C(5)-C(6)-H(6B)	109.6
H(6A)-C(6)-H(6B)	108.1
N(3)-C(7)-C(8)	114.87(16)
N(3)-C(7)-H(7A)	108.5
C(8)-C(7)-H(7A)	108.5
N(3)-C(7)-H(7B)	108.5
C(8)-C(7)-H(7B)	108.5
H(7A)-C(7)-H(7B)	107.5
N(4)-C(8)-C(9)	121.33(18)
N(4)-C(8)-C(7)	118.45(16)
C(9)-C(8)-C(7)	120.19(18)
C(10)-C(9)-C(8)	119.47(19)
C(10)-C(9)-H(9)	120.3
C(8)-C(9)-H(9)	120.3
C(9)-C(10)-C(11)	118.84(19)
C(9)-C(10)-H(10)	120.6
C(11)-C(10)-H(10)	120.6
C(12)-C(11)-C(10)	118.88(19)
C(12)-C(11)-H(11)	120.6
C(10)-C(11)-H(11)	120.6
N(4)-C(12)-C(11)	122.44(19)
N(4)-C(12)-H(12)	118.8
C(11)-C(12)-H(12)	118.8
N(3)-C(13)-C(14)	111.94(15)
N(3)-C(13)-H(13A)	109.2
C(14)-C(13)-H(13A)	109.2
N(3)-C(13)-H(13B)	109.2
C(14)-C(13)-H(13B)	109.2
H(13A)-C(13)-H(13B)	107.9
N(5)-C(14)-C(15)	121.42(18)
N(5)-C(14)-C(13)	117.19(16)
C(15)-C(14)-C(13)	121.20(18)
C(16)-C(15)-C(14)	119.18(19)
C(16)-C(15)-H(15)	120.4

SUPPORTING INFORMATION

C(14)-C(15)-H(15)	120.4
C(17)-C(16)-C(15)	119.49(18)
C(17)-C(16)-H(16)	120.3
C(15)-C(16)-H(16)	120.3
C(16)-C(17)-C(18)	118.5(2)
C(16)-C(17)-H(17)	120.7
C(18)-C(17)-H(17)	120.7
N(5)-C(18)-C(17)	122.21(19)
N(5)-C(18)-H(18)	118.9
C(17)-C(18)-H(18)	118.9
F(3)-C(19)-F(2)	107.90(18)
F(3)-C(19)-F(1)	107.53(16)
F(2)-C(19)-F(1)	107.92(17)
F(3)-C(19)-S(1)	111.17(14)
F(2)-C(19)-S(1)	111.01(14)
F(1)-C(19)-S(1)	111.15(15)
F(6)-C(20)-F(4)	107.64(16)
F(6)-C(20)-F(5)	107.57(17)
F(4)-C(20)-F(5)	107.98(18)
F(6)-C(20)-S(2)	111.29(15)
F(4)-C(20)-S(2)	110.88(15)
F(5)-C(20)-S(2)	111.31(13)

SUPPORTING INFORMATION

Table S5. Anisotropic displacement parameters ($\text{\AA}^2 \times 10^3$) for complex **1**.

The anisotropic displacement factor exponent takes the form:

$$-2\pi^2 [h^2 a^{*2} U_{11} + \dots + 2 h k a^* b^* U_{12}]$$

	U11	U22	U33	U23	U13	U12
Fe(1)	12(1)	17(1)	10(1)	1(1)	1(1)	-6(1)
S(1)	16(1)	14(1)	11(1)	3(1)	-1(1)	-6(1)
S(2)	13(1)	20(1)	16(1)	2(1)	-1(1)	-3(1)
F(1)	33(1)	33(1)	38(1)	22(1)	-1(1)	-15(1)
F(2)	39(1)	17(1)	50(1)	-4(1)	-6(1)	3(1)
F(3)	22(1)	38(1)	36(1)	14(1)	-13(1)	-8(1)
F(4)	34(1)	57(1)	17(1)	2(1)	2(1)	-19(1)
F(5)	16(1)	29(1)	33(1)	4(1)	4(1)	-4(1)
F(6)	30(1)	29(1)	41(1)	11(1)	-3(1)	-15(1)
N(1)	18(1)	29(1)	15(1)	0(1)	1(1)	-11(1)
N(2)	18(1)	21(1)	13(1)	5(1)	-2(1)	-11(1)
N(3)	13(1)	14(1)	12(1)	2(1)	1(1)	-5(1)
N(4)	17(1)	15(1)	13(1)	3(1)	1(1)	-6(1)
N(5)	14(1)	16(1)	14(1)	0(1)	-2(1)	-4(1)
O(1)	24(1)	62(1)	68(1)	-26(1)	22(1)	-17(1)
O(2)	15(1)	23(1)	14(1)	-2(1)	1(1)	-7(1)
O(3)	32(1)	19(1)	16(1)	-2(1)	-2(1)	-7(1)
O(4)	24(1)	30(1)	18(1)	5(1)	1(1)	-15(1)
O(5)	19(1)	23(1)	32(1)	6(1)	-4(1)	-3(1)
O(6)	21(1)	22(1)	28(1)	0(1)	3(1)	-8(1)
O(7)	19(1)	37(1)	19(1)	-3(1)	-2(1)	-5(1)
C(1)	24(1)	31(1)	15(1)	4(1)	-1(1)	-18(1)
C(2)	34(1)	31(1)	18(1)	10(1)	-8(1)	-24(1)
C(3)	34(1)	21(1)	25(1)	8(1)	-12(1)	-16(1)
C(4)	23(1)	18(1)	22(1)	3(1)	-7(1)	-9(1)
C(5)	16(1)	19(1)	14(1)	3(1)	-4(1)	-8(1)
C(6)	17(1)	13(1)	16(1)	0(1)	4(1)	-4(1)
C(7)	13(1)	27(1)	17(1)	-2(1)	-1(1)	-6(1)
C(8)	12(1)	11(1)	16(1)	5(1)	0(1)	-4(1)
C(9)	17(1)	19(1)	19(1)	1(1)	-3(1)	-6(1)
C(10)	24(1)	30(1)	19(1)	-2(1)	-6(1)	-8(1)
C(11)	22(1)	31(1)	17(1)	-6(1)	2(1)	-5(1)
C(12)	18(1)	20(1)	14(1)	1(1)	1(1)	-5(1)
C(13)	18(1)	16(1)	14(1)	4(1)	4(1)	-6(1)
C(14)	18(1)	16(1)	12(1)	2(1)	-2(1)	-7(1)
C(15)	24(1)	18(1)	16(1)	3(1)	-2(1)	-9(1)
C(16)	30(1)	18(1)	20(1)	6(1)	-7(1)	-9(1)
C(17)	24(1)	15(1)	24(1)	0(1)	-7(1)	-2(1)
C(18)	17(1)	20(1)	16(1)	-2(1)	-3(1)	-3(1)
C(19)	21(1)	20(1)	25(1)	6(1)	-2(1)	-7(1)
C(20)	21(1)	27(1)	20(1)	5(1)	-3(1)	-8(1)

SUPPORTING INFORMATION**Table S6.** Hydrogen coordinates ($x \times 10^4$) and isotropic displacement parameters ($\text{\AA}^2 \times 10^3$) for complex **1**.

	x	y	z	U(eq)
H(1)	3200	4057	8337	25
H(2)	4316	1354	8565	30
H(3)	6804	-87	7951	30
H(4)	8095	1209	7091	25
H(6A)	8286	3764	6639	19
H(6B)	6677	4314	6147	19
H(7A)	8426	6519	7351	23
H(7B)	8428	4863	7690	23
H(9)	8815	6725	8812	22
H(10)	7401	7832	9953	30
H(11)	4569	8466	10063	29
H(12)	3263	7953	9048	21
H(13A)	6480	6579	5774	20
H(13B)	7836	6993	6186	20
H(15)	6687	9750	5628	23
H(16)	4636	12237	5718	27
H(17)	2330	12551	6531	27
H(18)	2134	10369	7226	22

SUPPORTING INFORMATION

Table S7. Torsion angles [deg] for complex **1**.

O(3)-S(1)-O(2)-Fe(1)	-146.26(10)
O(4)-S(1)-O(2)-Fe(1)	-8.84(14)
C(19)-S(1)-O(2)-Fe(1)	102.81(12)
C(5)-N(2)-C(1)-C(2)	0.4(3)
Fe(1)-N(2)-C(1)-C(2)	-177.76(14)
N(2)-C(1)-C(2)-C(3)	0.3(3)
C(1)-C(2)-C(3)-C(4)	-0.9(3)
C(2)-C(3)-C(4)-C(5)	0.6(3)
C(1)-N(2)-C(5)-C(4)	-0.7(3)
Fe(1)-N(2)-C(5)-C(4)	177.65(14)
C(1)-N(2)-C(5)-C(6)	177.01(16)
Fe(1)-N(2)-C(5)-C(6)	-4.6(2)
C(3)-C(4)-C(5)-N(2)	0.2(3)
C(3)-C(4)-C(5)-C(6)	-177.41(17)
C(13)-N(3)-C(6)-C(5)	-156.18(16)
C(7)-N(3)-C(6)-C(5)	79.09(19)
Fe(1)-N(3)-C(6)-C(5)	-39.63(17)
N(2)-C(5)-C(6)-N(3)	31.0(2)
C(4)-C(5)-C(6)-N(3)	-151.26(17)
C(13)-N(3)-C(7)-C(8)	110.28(18)
C(6)-N(3)-C(7)-C(8)	-125.74(17)
Fe(1)-N(3)-C(7)-C(8)	-8.72(19)
C(12)-N(4)-C(8)-C(9)	-0.1(3)
Fe(1)-N(4)-C(8)-C(9)	176.60(13)
C(12)-N(4)-C(8)-C(7)	177.94(17)
Fe(1)-N(4)-C(8)-C(7)	-5.4(2)
N(3)-C(7)-C(8)-N(4)	9.7(2)
N(3)-C(7)-C(8)-C(9)	-172.21(16)
N(4)-C(8)-C(9)-C(10)	0.0(3)
C(7)-C(8)-C(9)-C(10)	-177.97(18)
C(8)-C(9)-C(10)-C(11)	-0.2(3)
C(9)-C(10)-C(11)-C(12)	0.3(3)
C(8)-N(4)-C(12)-C(11)	0.3(3)
Fe(1)-N(4)-C(12)-C(11)	-176.11(15)
C(10)-C(11)-C(12)-N(4)	-0.4(3)
C(6)-N(3)-C(13)-C(14)	150.06(16)
C(7)-N(3)-C(13)-C(14)	-86.26(19)
Fe(1)-N(3)-C(13)-C(14)	33.95(17)
C(18)-N(5)-C(14)-C(15)	0.1(3)
Fe(1)-N(5)-C(14)-C(15)	177.60(14)
C(18)-N(5)-C(14)-C(13)	-175.01(16)
Fe(1)-N(5)-C(14)-C(13)	2.5(2)
N(3)-C(13)-C(14)-N(5)	-25.7(2)
N(3)-C(13)-C(14)-C(15)	159.15(17)
N(5)-C(14)-C(15)-C(16)	-1.3(3)
C(13)-C(14)-C(15)-C(16)	173.60(17)
C(14)-C(15)-C(16)-C(17)	1.3(3)
C(15)-C(16)-C(17)-C(18)	-0.2(3)
C(14)-N(5)-C(18)-C(17)	1.1(3)
Fe(1)-N(5)-C(18)-C(17)	-176.11(14)
C(16)-C(17)-C(18)-N(5)	-1.1(3)
O(3)-S(1)-C(19)-F(3)	60.15(17)
O(4)-S(1)-C(19)-F(3)	-63.20(17)

SUPPORTING INFORMATION

O(2)-S(1)-C(19)-F(3)	177.72(14)
O(3)-S(1)-C(19)-F(2)	-179.73(14)
O(4)-S(1)-C(19)-F(2)	56.92(16)
O(2)-S(1)-C(19)-F(2)	-62.16(16)
O(3)-S(1)-C(19)-F(1)	-59.60(16)
O(4)-S(1)-C(19)-F(1)	177.05(14)
O(2)-S(1)-C(19)-F(1)	57.97(16)
O(6)-S(2)-C(20)-F(6)	-176.29(13)
O(5)-S(2)-C(20)-F(6)	-55.92(16)
O(7)-S(2)-C(20)-F(6)	63.91(16)
O(6)-S(2)-C(20)-F(4)	-56.50(16)
O(5)-S(2)-C(20)-F(4)	63.86(17)
O(7)-S(2)-C(20)-F(4)	-176.31(15)
O(6)-S(2)-C(20)-F(5)	63.73(16)
O(5)-S(2)-C(20)-F(5)	-175.91(14)
O(7)-S(2)-C(20)-F(5)	-56.08(16)

SUPPORTING INFORMATION

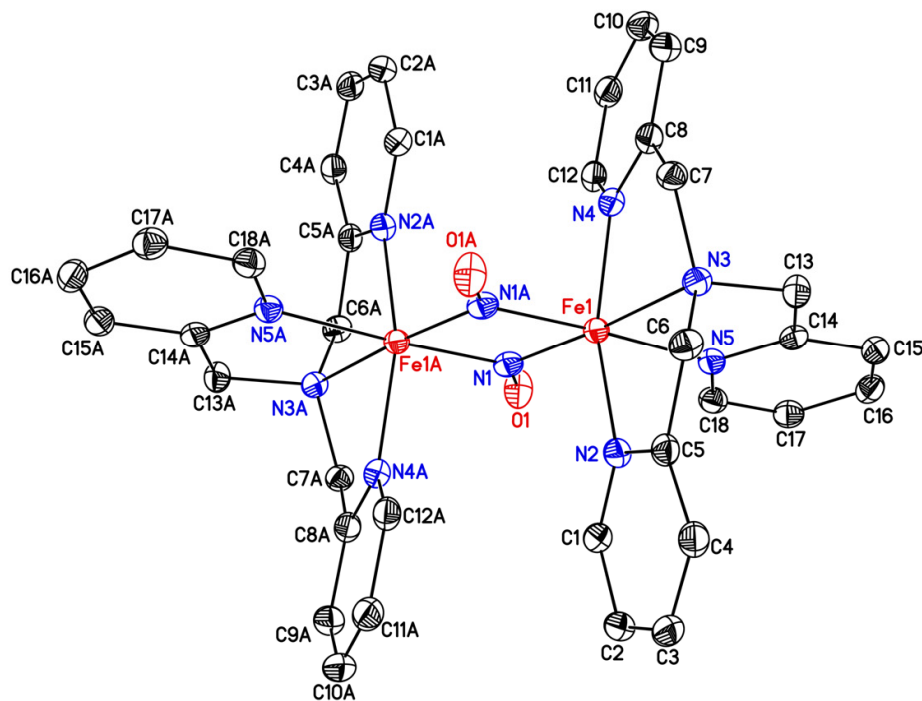


Figure S25. Crystal structure of complex **2** with ellipsoids drawn at 50% probability. The triflate counter anions, solvent molecules, and hydrogen atoms are omitted for clarity. The atomic labelling scheme is shown. Important structural parameters:

Table S8. Important crystal parameters of complex **2**.

Selected bonds/angles	Å/deg.
N1–O1 = N1A–O1A	1.247
Fe1–N1	1.820
Fe1A–N1	1.876
Fe1–N1–Fe1A	103.1
Fe1–N1–O1	129.0
Fe1A–N1–O1	127.7
Fe1–Fe1A	2.895
N1–N1A	2.298

SUPPORTING INFORMATION**Table S9.** Crystal data and structure refinement for complex 2.

Identification code	hd1157b
Empirical formula	C38 H36 F6 Fe2 N10 O8 S2
Formula weight	1050.59
Temperature	85(2) K
Wavelength	1.54184 Å
Crystal system, space group	Monoclinic, P2(1)/c
Unit cell dimensions	a = 9.17870(10) Å alpha = 90 deg. b = 16.2396(2) Å beta = 102.3120(10) deg. c = 14.3377(2) Å gamma = 90 deg.
Volume	2088.00(5) Å ³
Z, Calculated density	2, 1.671 Mg/m ³
Absorption coefficient	7.330 mm ⁻¹
F(000)	1072
Crystal size	0.120 x 0.100 x 0.100 mm
Theta range for data collection	4.168 to 69.162 deg.
Limiting indices	-11<=h<=11, -19<=k<=19, -17<=l<=17
Reflections collected / unique	31405 / 3875 [R(int) = 0.0455]
Completeness to theta = 67.684	99.9 %
Absorption correction	Semi-empirical from equivalents
Max. and min. transmission	1.00000 and 0.55642
Refinement method	Full-matrix least-squares on F ²
Data / restraints / parameters	3875 / 0 / 299
Goodness-of-fit on F ²	1.043
Final R indices [I>2σ(I)]	R1 = 0.0314, wR2 = 0.0847
R indices (all data)	R1 = 0.0323, wR2 = 0.0856
Extinction coefficient	0.00062(9)
Largest diff. peak and hole	0.376 and -0.625 e.Å ³

SUPPORTING INFORMATION

Table S10. Atomic coordinates ($x \times 10^4$) and equivalent isotropic displacement parameters ($\text{\AA}^2 \times 10^3$) for complex **2**.
U(eq) is defined as one third of the trace of the orthogonalized Uij tensor.

	x	y	z	U(eq)
Fe(1)	5346(1)	4894(1)	6026(1)	14(1)
S(1)	82(1)	8639(1)	5058(1)	25(1)
F(1)	-1101(1)	7260(1)	5516(1)	33(1)
F(2)	1281(2)	7273(1)	5843(1)	63(1)
F(3)	71(2)	7128(1)	4388(1)	57(1)
O(1)	2401(2)	4951(1)	5025(1)	25(1)
O(2)	1470(2)	8796(1)	4784(1)	48(1)
O(3)	2(2)	8931(1)	5989(1)	32(1)
O(4)	-1255(2)	8775(1)	4342(1)	41(1)
N(1)	3758(2)	4998(1)	5028(1)	17(1)
N(2)	5680(2)	6068(1)	6373(1)	17(1)
N(3)	7265(2)	4759(1)	7087(1)	17(1)
N(4)	5477(2)	3672(1)	6062(1)	17(1)
N(5)	4304(2)	4823(1)	7163(1)	16(1)
C(1)	4651(2)	6670(1)	6188(1)	19(1)
C(2)	4957(2)	7469(1)	6500(1)	21(1)
C(3)	6361(2)	7650(1)	7038(1)	22(1)
C(4)	7410(2)	7028(1)	7254(1)	20(1)
C(5)	7048(2)	6243(1)	6907(1)	18(1)
C(6)	8126(2)	5532(1)	7073(1)	19(1)
C(7)	8016(2)	4016(1)	6802(1)	18(1)
C(8)	6840(2)	3369(1)	6476(1)	19(1)
C(9)	7096(2)	2532(1)	6568(1)	22(1)
C(10)	5939(2)	1986(1)	6237(1)	24(1)
C(11)	4537(2)	2294(1)	5839(1)	22(1)
C(12)	4348(2)	3140(1)	5761(1)	19(1)
C(13)	6878(2)	4633(1)	8037(1)	19(1)
C(14)	5239(2)	4689(1)	8013(1)	17(1)
C(15)	4730(2)	4594(1)	8855(1)	19(1)
C(16)	3219(2)	4653(1)	8833(1)	20(1)
C(17)	2258(2)	4814(1)	7962(1)	20(1)
C(18)	2832(2)	4891(1)	7149(1)	19(1)
C(19)	88(2)	7521(1)	5212(2)	31(1)

SUPPORTING INFORMATION

Table S11. Bond lengths [Å] and angles [deg] for complex **2**.

Fe(1)-N(1)	1.8202(17)
Fe(1)-N(1)#1	1.8757(17)
Fe(1)-N(2)	1.9769(15)
Fe(1)-N(4)	1.9892(16)
Fe(1)-N(5)	2.0619(16)
Fe(1)-N(3)	2.0787(15)
S(1)-O(3)	1.4335(14)
S(1)-O(2)	1.4335(16)
S(1)-O(4)	1.4389(16)
S(1)-C(19)	1.829(2)
F(1)-C(19)	1.329(2)
F(2)-C(19)	1.326(3)
F(3)-C(19)	1.340(3)
O(1)-N(1)	1.247(2)
N(2)-C(1)	1.346(2)
N(2)-C(5)	1.354(2)
N(3)-C(6)	1.486(2)
N(3)-C(7)	1.489(2)
N(3)-C(13)	1.493(2)
N(4)-C(12)	1.347(2)
N(4)-C(8)	1.357(2)
N(5)-C(14)	1.350(2)
N(5)-C(18)	1.352(2)
C(1)-C(2)	1.381(3)
C(1)-H(1)	0.9500
C(2)-C(3)	1.385(3)
C(2)-H(2)	0.9500
C(3)-C(4)	1.383(3)
C(3)-H(3)	0.9500
C(4)-C(5)	1.383(2)
C(4)-H(4)	0.9500
C(5)-C(6)	1.507(2)
C(6)-H(6A)	0.9900
C(6)-H(6B)	0.9900
C(7)-C(8)	1.509(2)
C(7)-H(7A)	0.9900
C(7)-H(7B)	0.9900
C(8)-C(9)	1.380(3)
C(9)-C(10)	1.388(3)
C(9)-H(9)	0.9500
C(10)-C(11)	1.384(3)
C(10)-H(10)	0.9500
C(11)-C(12)	1.386(3)
C(11)-H(11)	0.9500
C(12)-H(12)	0.9500
C(13)-C(14)	1.500(2)
C(13)-H(13A)	0.9900
C(13)-H(13B)	0.9900
C(14)-C(15)	1.393(3)
C(15)-C(16)	1.384(3)
C(15)-H(15)	0.9500
C(16)-C(17)	1.391(3)
C(16)-H(16)	0.9500

SUPPORTING INFORMATION

C(17)-C(18)	1.384(3)
C(17)-H(17)	0.9500
C(18)-H(18)	0.9500
N(1)-Fe(1)-N(1)#1	76.88(8)
N(1)-Fe(1)-N(2)	99.41(6)
N(1)#1-Fe(1)-N(2)	92.39(6)
N(1)-Fe(1)-N(4)	98.43(6)
N(1)#1-Fe(1)-N(4)	94.55(6)
N(2)-Fe(1)-N(4)	161.92(6)
N(1)-Fe(1)-N(5)	101.43(7)
N(1)#1-Fe(1)-N(5)	177.39(6)
N(2)-Fe(1)-N(5)	85.90(6)
N(4)-Fe(1)-N(5)	87.66(6)
N(1)-Fe(1)-N(3)	175.42(7)
N(1)#1-Fe(1)-N(3)	98.68(7)
N(2)-Fe(1)-N(3)	81.75(6)
N(4)-Fe(1)-N(3)	80.70(6)
N(5)-Fe(1)-N(3)	83.05(6)
O(3)-S(1)-O(2)	114.93(10)
O(3)-S(1)-O(4)	114.08(10)
O(2)-S(1)-O(4)	116.78(11)
O(3)-S(1)-C(19)	102.44(10)
O(2)-S(1)-C(19)	103.22(10)
O(4)-S(1)-C(19)	102.62(9)
O(1)-N(1)-Fe(1)	128.97(13)
O(1)-N(1)-Fe(1)#1	127.74(13)
Fe(1)-N(1)-Fe(1)#1	103.12(8)
C(1)-N(2)-C(5)	119.03(15)
C(1)-N(2)-Fe(1)	125.91(12)
C(5)-N(2)-Fe(1)	114.85(11)
C(6)-N(3)-C(7)	113.68(14)
C(6)-N(3)-C(13)	111.01(14)
C(7)-N(3)-C(13)	110.69(13)
C(6)-N(3)-Fe(1)	105.71(10)
C(7)-N(3)-Fe(1)	104.78(10)
C(13)-N(3)-Fe(1)	110.67(11)
C(12)-N(4)-C(8)	118.81(15)
C(12)-N(4)-Fe(1)	126.41(12)
C(8)-N(4)-Fe(1)	114.70(12)
C(14)-N(5)-C(18)	117.90(16)
C(14)-N(5)-Fe(1)	114.18(12)
C(18)-N(5)-Fe(1)	127.92(13)
N(2)-C(1)-C(2)	122.20(17)
N(2)-C(1)-H(1)	118.9
C(2)-C(1)-H(1)	118.9
C(1)-C(2)-C(3)	118.70(17)
C(1)-C(2)-H(2)	120.6
C(3)-C(2)-H(2)	120.6
C(4)-C(3)-C(2)	119.38(17)
C(4)-C(3)-H(3)	120.3
C(2)-C(3)-H(3)	120.3
C(5)-C(4)-C(3)	119.30(17)
C(5)-C(4)-H(4)	120.3
C(3)-C(4)-H(4)	120.3
N(2)-C(5)-C(4)	121.34(16)
N(2)-C(5)-C(6)	115.25(15)

SUPPORTING INFORMATION

C(4)-C(5)-C(6)	123.40(16)
N(3)-C(6)-C(5)	108.42(14)
N(3)-C(6)-H(6A)	110.0
C(5)-C(6)-H(6A)	110.0
N(3)-C(6)-H(6B)	110.0
C(5)-C(6)-H(6B)	110.0
H(6A)-C(6)-H(6B)	108.4
N(3)-C(7)-C(8)	107.86(13)
N(3)-C(7)-H(7A)	110.1
C(8)-C(7)-H(7A)	110.1
N(3)-C(7)-H(7B)	110.1
C(8)-C(7)-H(7B)	110.1
H(7A)-C(7)-H(7B)	108.4
N(4)-C(8)-C(9)	121.42(17)
N(4)-C(8)-C(7)	114.54(15)
C(9)-C(8)-C(7)	124.04(16)
C(8)-C(9)-C(10)	119.56(17)
C(8)-C(9)-H(9)	120.2
C(10)-C(9)-H(9)	120.2
C(11)-C(10)-C(9)	119.14(17)
C(11)-C(10)-H(10)	120.4
C(9)-C(10)-H(10)	120.4
C(10)-C(11)-C(12)	118.68(17)
C(10)-C(11)-H(11)	120.7
C(12)-C(11)-H(11)	120.7
N(4)-C(12)-C(11)	122.34(17)
N(4)-C(12)-H(12)	118.8
C(11)-C(12)-H(12)	118.8
N(3)-C(13)-C(14)	113.76(14)
N(3)-C(13)-H(13A)	108.8
C(14)-C(13)-H(13A)	108.8
N(3)-C(13)-H(13B)	108.8
C(14)-C(13)-H(13B)	108.8
H(13A)-C(13)-H(13B)	107.7
N(5)-C(14)-C(15)	122.28(16)
N(5)-C(14)-C(13)	118.17(15)
C(15)-C(14)-C(13)	119.54(15)
C(16)-C(15)-C(14)	119.46(16)
C(16)-C(15)-H(15)	120.3
C(14)-C(15)-H(15)	120.3
C(15)-C(16)-C(17)	118.31(17)
C(15)-C(16)-H(16)	120.8
C(17)-C(16)-H(16)	120.8
C(18)-C(17)-C(16)	119.42(17)
C(18)-C(17)-H(17)	120.3
C(16)-C(17)-H(17)	120.3
N(5)-C(18)-C(17)	122.60(17)
N(5)-C(18)-H(18)	118.7
C(17)-C(18)-H(18)	118.7
F(2)-C(19)-F(1)	107.22(18)
F(2)-C(19)-F(3)	108.05(18)
F(1)-C(19)-F(3)	106.33(17)
F(2)-C(19)-S(1)	111.44(15)
F(1)-C(19)-S(1)	112.01(14)
F(3)-C(19)-S(1)	111.52(16)

SUPPORTING INFORMATION

Symmetry transformations used to generate equivalent atoms:
#1 -x+1,-y+1,-z+1

SUPPORTING INFORMATION**Table S12.** Anisotropic displacement parameters ($\text{\AA}^2 \times 10^3$) for complex **2**.

The anisotropic displacement factor exponent takes the form:

$$-2\pi^2 [h^2 a^{*2} U_{11} + \dots + 2 h k a^* b^* U_{12}]$$

	U11	U22	U33	U23	U13	U12
Fe(1)	14(1)	14(1)	14(1)	0(1)	2(1)	1(1)
S(1)	28(1)	27(1)	21(1)	-5(1)	8(1)	-5(1)
F(1)	28(1)	37(1)	35(1)	8(1)	11(1)	-3(1)
F(2)	28(1)	46(1)	106(1)	17(1)	-6(1)	9(1)
F(3)	85(1)	32(1)	70(1)	-19(1)	51(1)	-14(1)
O(1)	16(1)	40(1)	19(1)	1(1)	4(1)	0(1)
O(2)	55(1)	38(1)	65(1)	-20(1)	42(1)	-18(1)
O(3)	25(1)	44(1)	25(1)	-12(1)	4(1)	0(1)
O(4)	57(1)	32(1)	27(1)	5(1)	-10(1)	-11(1)
N(1)	18(1)	14(1)	20(1)	-2(1)	5(1)	-1(1)
N(2)	18(1)	17(1)	16(1)	1(1)	5(1)	1(1)
N(3)	17(1)	16(1)	17(1)	-1(1)	4(1)	1(1)
N(4)	19(1)	18(1)	15(1)	-1(1)	5(1)	0(1)
N(5)	18(1)	15(1)	16(1)	0(1)	3(1)	0(1)
C(1)	21(1)	19(1)	17(1)	0(1)	6(1)	2(1)
C(2)	28(1)	18(1)	20(1)	2(1)	8(1)	5(1)
C(3)	33(1)	16(1)	19(1)	-2(1)	8(1)	-2(1)
C(4)	24(1)	20(1)	16(1)	0(1)	4(1)	-3(1)
C(5)	21(1)	18(1)	15(1)	1(1)	5(1)	-1(1)
C(6)	17(1)	18(1)	20(1)	-3(1)	3(1)	-2(1)
C(7)	16(1)	18(1)	18(1)	-1(1)	2(1)	3(1)
C(8)	20(1)	21(1)	15(1)	0(1)	4(1)	1(1)
C(9)	24(1)	20(1)	22(1)	2(1)	7(1)	4(1)
C(10)	33(1)	16(1)	24(1)	-1(1)	10(1)	0(1)
C(11)	29(1)	19(1)	19(1)	-2(1)	7(1)	-4(1)
C(12)	22(1)	20(1)	14(1)	0(1)	4(1)	-2(1)
C(13)	21(1)	22(1)	15(1)	0(1)	3(1)	0(1)
C(14)	22(1)	12(1)	17(1)	-2(1)	4(1)	0(1)
C(15)	22(1)	16(1)	17(1)	-1(1)	2(1)	-1(1)
C(16)	25(1)	18(1)	19(1)	-2(1)	9(1)	-3(1)
C(17)	18(1)	20(1)	23(1)	0(1)	6(1)	1(1)
C(18)	19(1)	18(1)	20(1)	1(1)	3(1)	2(1)
C(19)	25(1)	31(1)	39(1)	0(1)	14(1)	1(1)

SUPPORTING INFORMATION

Table S13. Hydrogen coordinates ($\times 10^4$) and isotropic displacement parameters ($\text{\AA}^2 \times 10^3$) for complex **2**.

	x	y	z	U(eq)
H(1)	3682	6541	5831	23
H(2)	4219	7886	6348	26
H(3)	6602	8195	7256	27
H(4)	8369	7140	7637	24
H(6A)	8690	5508	6557	22
H(6B)	8846	5603	7688	22
H(7A)	8772	3809	7351	21
H(7B)	8524	4154	6279	21
H(9)	8059	2332	6857	26
H(10)	6106	1409	6282	28
H(11)	3721	1932	5623	27
H(12)	3388	3352	5486	23
H(13A)	7406	5051	8487	23
H(13B)	7242	4084	8284	23
H(15)	5415	4489	9440	23
H(16)	2847	4585	9398	24
H(17)	1218	4871	7927	24
H(18)	2164	4997	6557	23

SUPPORTING INFORMATION

Table S14. Torsion angles [deg] for complex 2.

N(1)#1-Fe(1)-N(1)-O(1)	175.40(19)
N(2)-Fe(1)-N(1)-O(1)	-94.32(15)
N(4)-Fe(1)-N(1)-O(1)	82.66(15)
N(5)-Fe(1)-N(1)-O(1)	-6.63(16)
N(1)#1-Fe(1)-N(1)-Fe(1)#1	0.0
N(2)-Fe(1)-N(1)-Fe(1)#1	90.28(7)
N(4)-Fe(1)-N(1)-Fe(1)#1	-92.74(7)
N(5)-Fe(1)-N(1)-Fe(1)#1	177.96(6)
C(5)-N(2)-C(1)-C(2)	2.1(3)
Fe(1)-N(2)-C(1)-C(2)	176.53(13)
N(2)-C(1)-C(2)-C(3)	-1.4(3)
C(1)-C(2)-C(3)-C(4)	-0.5(3)
C(2)-C(3)-C(4)-C(5)	1.7(3)
C(1)-N(2)-C(5)-C(4)	-0.9(2)
Fe(1)-N(2)-C(5)-C(4)	-175.89(13)
C(1)-N(2)-C(5)-C(6)	-179.74(15)
Fe(1)-N(2)-C(5)-C(6)	5.23(19)
C(3)-C(4)-C(5)-N(2)	-1.0(3)
C(3)-C(4)-C(5)-C(6)	177.76(16)
C(7)-N(3)-C(6)-C(5)	153.58(14)
C(13)-N(3)-C(6)-C(5)	-80.85(17)
Fe(1)-N(3)-C(6)-C(5)	39.21(15)
N(2)-C(5)-C(6)-N(3)	-30.9(2)
C(4)-C(5)-C(6)-N(3)	150.27(16)
C(6)-N(3)-C(7)-C(8)	-158.17(14)
C(13)-N(3)-C(7)-C(8)	76.09(17)
Fe(1)-N(3)-C(7)-C(8)	-43.25(15)
C(12)-N(4)-C(8)-C(9)	1.9(2)
Fe(1)-N(4)-C(8)-C(9)	178.83(14)
C(12)-N(4)-C(8)-C(7)	-178.93(15)
Fe(1)-N(4)-C(8)-C(7)	-1.97(19)
N(3)-C(7)-C(8)-N(4)	31.5(2)
N(3)-C(7)-C(8)-C(9)	-149.37(17)
N(4)-C(8)-C(9)-C(10)	-0.3(3)
C(7)-C(8)-C(9)-C(10)	-179.46(16)
C(8)-C(9)-C(10)-C(11)	-1.5(3)
C(9)-C(10)-C(11)-C(12)	1.8(3)
C(8)-N(4)-C(12)-C(11)	-1.6(2)
Fe(1)-N(4)-C(12)-C(11)	-178.16(13)
C(10)-C(11)-C(12)-N(4)	-0.2(3)
C(6)-N(3)-C(13)-C(14)	113.30(16)
C(7)-N(3)-C(13)-C(14)	-119.47(16)
Fe(1)-N(3)-C(13)-C(14)	-3.76(18)
C(18)-N(5)-C(14)-C(15)	2.2(2)
Fe(1)-N(5)-C(14)-C(15)	-177.69(13)
C(18)-N(5)-C(14)-C(13)	-178.51(15)
Fe(1)-N(5)-C(14)-C(13)	1.64(19)
N(3)-C(13)-C(14)-N(5)	1.5(2)
N(3)-C(13)-C(14)-C(15)	-179.16(15)
N(5)-C(14)-C(15)-C(16)	-1.3(3)
C(13)-C(14)-C(15)-C(16)	179.42(16)
C(14)-C(15)-C(16)-C(17)	-0.6(3)
C(15)-C(16)-C(17)-C(18)	1.5(3)
C(14)-N(5)-C(18)-C(17)	-1.3(2)

SUPPORTING INFORMATION

Fe(1)-N(5)-C(18)-C(17)	178.57(13)
C(16)-C(17)-C(18)-N(5)	-0.5(3)
O(3)-S(1)-C(19)-F(2)	-62.86(17)
O(2)-S(1)-C(19)-F(2)	56.82(18)
O(4)-S(1)-C(19)-F(2)	178.61(16)
O(3)-S(1)-C(19)-F(1)	57.25(17)
O(2)-S(1)-C(19)-F(1)	176.94(16)
O(4)-S(1)-C(19)-F(1)	-61.27(18)
O(3)-S(1)-C(19)-F(3)	176.29(14)
O(2)-S(1)-C(19)-F(3)	-64.02(17)
O(4)-S(1)-C(19)-F(3)	57.77(17)

Symmetry transformations used to generate equivalent atoms:

#1 -x+1,-y+1,-z+1

SUPPORTING INFORMATION

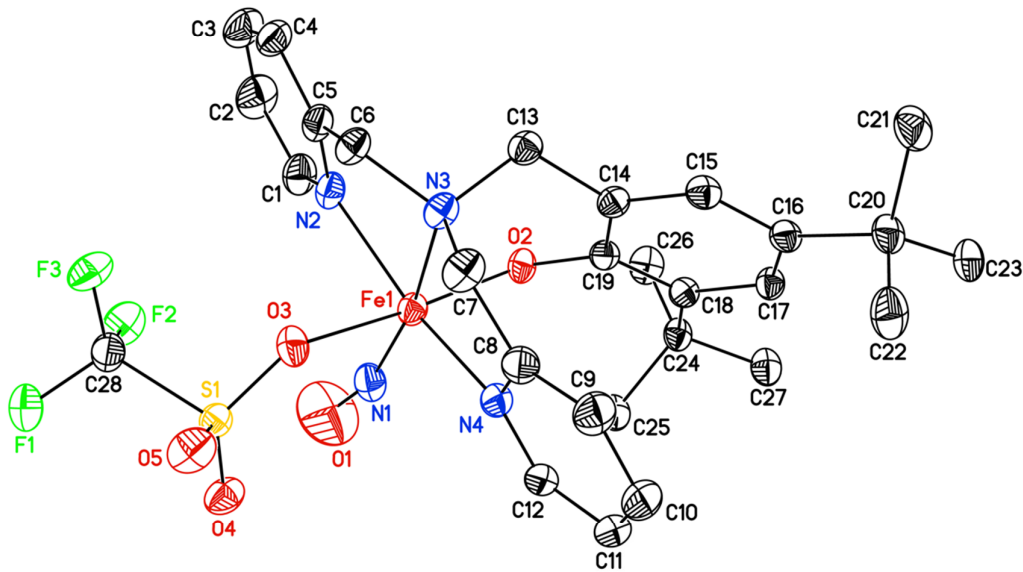


Figure S26. Crystal structure of complex **3** with ellipsoids drawn at 50% probability. Solvent molecules, and hydrogen atoms are omitted for clarity. The atomic labelling scheme is shown. Important structural parameters:

Table S15. Important crystal parameters of complex **3**.

Selected bonds/angles	Å/deg.
Fe1–N1	1.777
N1–O1	1.100
Fe1–N2	2.131
Fe1–N3	2.216
Fe1–N4	2.151
Fe1–O2	1.953
F1–O3	2.231
Fe1–N1–O1	163

SUPPORTING INFORMATION**Table S16.** Crystal data and structure refinement for complex **3**.

Identification code	als3095
Empirical formula	C28 H34 F3 Fe N4 O5 S
Formula weight	651.50
Temperature	85(2) K
Wavelength	0.71073 Å
Crystal system, space group	Monoclinic, C2/c
Unit cell dimensions	a = 43.468(4) Å alpha = 90 deg. b = 10.1454(9) Å beta = 108.6170(10) deg. c = 14.5464(13) Å gamma = 90 deg.
Volume	6079.3(9) Å ³
Z, Calculated density	8, 1.424 Mg/m ³
Absorption coefficient	0.626 mm ⁻¹
F(000)	2712
Crystal size	0.310 x 0.140 x 0.020 mm
Theta range for data collection	1.977 to 28.315 deg.
Limiting indices	-57<=h<=57, -13<=k<=13, -19<=l<=19
Reflections collected / unique	58299 / 7563 [R(int) = 0.0659]
Completeness to theta = 25.242	100.0 %
Absorption correction	Semi-empirical from equivalents
Max. and min. transmission	0.9876 and 0.8295
Refinement method	Full-matrix least-squares on F ²
Data / restraints / parameters	7563 / 20 / 458
Goodness-of-fit on F ²	1.004
Final R indices [I>2σ(I)]	R1 = 0.0402, wR2 = 0.0928
R indices (all data)	R1 = 0.0623, wR2 = 0.1052
Extinction coefficient	n/a
Largest diff. peak and hole	0.814 and -0.428 e. Å ⁻³

SUPPORTING INFORMATION

Table S17. Atomic coordinates ($\times 10^4$) and equivalent isotropic displacement parameters ($\text{\AA}^2 \times 10^3$) for complex **3**.
U(eq) is defined as one third of the trace of the orthogonalized Uij tensor.

	x	y	z	U(eq)
Fe(1)	1036(1)	1595(1)	6551(1)	21(1)
O(1)	1165(1)	3905(2)	5624(2)	80(1)
O(2)	1434(1)	1372(1)	7642(1)	21(1)
S(1)	382(1)	1854(1)	4436(1)	21(1)
O(3)	551(2)	1422(7)	5415(6)	26(1)
O(4)	582(1)	2543(2)	3979(2)	30(1)
O(5)	166(1)	878(3)	3871(2)	34(1)
C(28)	115(1)	3130(3)	4638(2)	28(1)
F(1)	-71(1)	3648(3)	3804(2)	41(1)
F(2)	287(1)	4107(2)	5176(2)	34(1)
F(3)	-80(1)	2637(4)	5103(3)	34(1)
S(1A)	318(1)	2763(1)	5025(1)	21(1)
O(3A)	568(3)	1743(11)	5301(10)	22(2)
O(4A)	451(1)	4076(5)	5173(4)	30(1)
O(5A)	45(1)	2525(9)	5343(6)	32(2)
C(28A)	158(1)	2573(5)	3712(4)	23(1)
F(1A)	392(1)	2699(3)	3304(2)	28(1)
F(2A)	25(1)	1391(4)	3478(3)	33(1)
F(3A)	-69(1)	3466(5)	3324(3)	39(1)
N(1)	1157(1)	2946(2)	5969(1)	29(1)
N(2)	779(1)	2659(2)	7339(1)	24(1)
N(3)	789(1)	22(2)	7109(1)	22(1)
N(4)	1133(1)	-141(2)	5840(1)	24(1)
C(1)	841(1)	3915(2)	7639(2)	31(1)
C(2)	688(1)	4521(2)	8225(2)	40(1)
C(3)	468(1)	3805(2)	8527(2)	39(1)
C(4)	404(1)	2511(2)	8230(2)	31(1)
C(5)	560(1)	1969(2)	7626(1)	25(1)
C(6)	491(1)	592(2)	7231(2)	24(1)
C(7)	716(1)	-1092(2)	6417(2)	28(1)
C(8)	983(1)	-1255(2)	5971(1)	26(1)
C(9)	1063(1)	-2480(2)	5686(2)	32(1)
C(10)	1306(1)	-2563(2)	5269(2)	38(1)
C(11)	1462(1)	-1425(2)	5140(2)	36(1)
C(12)	1368(1)	-234(2)	5431(1)	28(1)
C(13)	1007(1)	-386(2)	8084(1)	22(1)
C(14)	1344(1)	-796(2)	8120(1)	20(1)
C(15)	1452(1)	-2070(2)	8377(1)	22(1)
C(16)	1770(1)	-2445(2)	8480(1)	21(1)
C(17)	1977(1)	-1462(2)	8352(1)	20(1)
C(18)	1881(1)	-158(2)	8100(1)	19(1)
C(19)	1552(1)	171(2)	7946(1)	19(1)
C(20)	1875(1)	-3889(2)	8665(2)	24(1)
C(21)	1744(1)	-4504(2)	9429(2)	35(1)
C(22)	1737(1)	-4640(2)	7699(2)	34(1)
C(23)	2244(1)	-4041(2)	9022(2)	27(1)
C(24)	2128(1)	898(2)	8041(1)	22(1)

SUPPORTING INFORMATION

C(25)	2031(1)	1555(2)	7034(2)	27(1)
C(26)	2146(1)	1947(2)	8821(2)	28(1)
C(27)	2472(1)	336(2)	8241(2)	28(1)

SUPPORTING INFORMATION

Table S18. Bond lengths [Å] and angles [deg] for complex 3.

Fe(1)-N(1)	1.7773(18)
Fe(1)-O(2)	1.9533(13)
Fe(1)-N(2)	2.1314(16)
Fe(1)-N(4)	2.1514(16)
Fe(1)-N(3)	2.2159(16)
Fe(1)-O(3)	2.231(6)
Fe(1)-O(3A)	2.259(9)
O(1)-N(1)	1.100(2)
O(2)-C(19)	1.341(2)
S(1)-O(5)	1.429(3)
S(1)-O(4)	1.434(2)
S(1)-O(3)	1.446(6)
S(1)-C(28)	1.826(3)
C(28)-F(1)	1.331(4)
C(28)-F(2)	1.335(4)
C(28)-F(3)	1.337(5)
S(1A)-O(5A)	1.427(7)
S(1A)-O(4A)	1.441(5)
S(1A)-O(3A)	1.459(11)
S(1A)-C(28A)	1.822(5)
C(28A)-F(3A)	1.324(6)
C(28A)-F(2A)	1.327(6)
C(28A)-F(1A)	1.341(5)
N(2)-C(1)	1.347(3)
N(2)-C(5)	1.349(3)
N(3)-C(7)	1.478(2)
N(3)-C(6)	1.480(2)
N(3)-C(13)	1.491(2)
N(4)-C(12)	1.342(3)
N(4)-C(8)	1.348(3)
C(1)-C(2)	1.380(3)
C(1)-H(1A)	0.9500
C(2)-C(3)	1.382(3)
C(2)-H(2A)	0.9500
C(3)-C(4)	1.383(3)
C(3)-H(3A)	0.9500
C(4)-C(5)	1.383(3)
C(4)-H(4A)	0.9500
C(5)-C(6)	1.505(3)
C(6)-H(6A)	0.9900
C(6)-H(6B)	0.9900
C(7)-C(8)	1.507(3)
C(7)-H(7A)	0.9900
C(7)-H(7B)	0.9900
C(8)-C(9)	1.389(3)
C(9)-C(10)	1.379(3)
C(9)-H(9A)	0.9500
C(10)-C(11)	1.381(3)
C(10)-H(10A)	0.9500
C(11)-C(12)	1.383(3)
C(11)-H(11A)	0.9500
C(12)-H(12A)	0.9500
C(13)-C(14)	1.505(3)

SUPPORTING INFORMATION

C(13)-H(13A)	0.9900
C(13)-H(13B)	0.9900
C(14)-C(15)	1.386(3)
C(14)-C(19)	1.413(2)
C(15)-C(16)	1.393(3)
C(15)-H(15A)	0.9500
C(16)-C(17)	1.396(2)
C(16)-C(20)	1.533(3)
C(17)-C(18)	1.401(2)
C(17)-H(17A)	0.9500
C(18)-C(19)	1.415(3)
C(18)-C(24)	1.538(2)
C(20)-C(23)	1.529(3)
C(20)-C(21)	1.534(3)
C(20)-C(22)	1.542(3)
C(21)-H(21A)	0.9800
C(21)-H(21B)	0.9800
C(21)-H(21C)	0.9800
C(22)-H(22A)	0.9800
C(22)-H(22B)	0.9800
C(22)-H(22C)	0.9800
C(23)-H(23A)	0.9800
C(23)-H(23B)	0.9800
C(23)-H(23C)	0.9800
C(24)-C(27)	1.536(3)
C(24)-C(26)	1.538(3)
C(24)-C(25)	1.541(3)
C(25)-H(25A)	0.9800
C(25)-H(25B)	0.9800
C(25)-H(25C)	0.9800
C(26)-H(26A)	0.9800
C(26)-H(26B)	0.9800
C(26)-H(26C)	0.9800
C(27)-H(27A)	0.9800
C(27)-H(27B)	0.9800
C(27)-H(27C)	0.9800
N(1)-Fe(1)-O(2)	98.95(7)
N(1)-Fe(1)-N(2)	98.73(7)
O(2)-Fe(1)-N(2)	95.86(6)
N(1)-Fe(1)-N(4)	105.62(7)
O(2)-Fe(1)-N(4)	92.09(6)
N(2)-Fe(1)-N(4)	152.85(6)
N(1)-Fe(1)-N(3)	169.06(7)
O(2)-Fe(1)-N(3)	91.46(6)
N(2)-Fe(1)-N(3)	76.70(6)
N(4)-Fe(1)-N(3)	77.19(6)
N(1)-Fe(1)-O(3)	93.56(15)
O(2)-Fe(1)-O(3)	167.26(13)
N(2)-Fe(1)-O(3)	84.5(3)
N(4)-Fe(1)-O(3)	82.2(3)
N(3)-Fe(1)-O(3)	76.21(15)
N(1)-Fe(1)-O(3A)	83.9(2)
O(2)-Fe(1)-O(3A)	177.0(2)
N(2)-Fe(1)-O(3A)	84.7(5)
N(4)-Fe(1)-O(3A)	86.1(4)
N(3)-Fe(1)-O(3A)	85.8(3)

SUPPORTING INFORMATION

C(19)-O(2)-Fe(1)	121.34(11)
O(5)-S(1)-O(4)	117.11(16)
O(5)-S(1)-O(3)	112.9(3)
O(4)-S(1)-O(3)	114.4(3)
O(5)-S(1)-C(28)	104.39(16)
O(4)-S(1)-C(28)	103.94(14)
O(3)-S(1)-C(28)	101.8(4)
S(1)-O(3)-Fe(1)	140.1(4)
F(1)-C(28)-F(2)	107.7(3)
F(1)-C(28)-F(3)	108.1(3)
F(2)-C(28)-F(3)	107.9(3)
F(1)-C(28)-S(1)	111.5(2)
F(2)-C(28)-S(1)	110.8(2)
F(3)-C(28)-S(1)	110.8(3)
O(5A)-S(1A)-O(4A)	116.4(4)
O(5A)-S(1A)-O(3A)	114.4(6)
O(4A)-S(1A)-O(3A)	112.8(5)
O(5A)-S(1A)-C(28A)	103.9(3)
O(4A)-S(1A)-C(28A)	104.9(3)
O(3A)-S(1A)-C(28A)	102.5(7)
S(1A)-O(3A)-Fe(1)	131.8(9)
F(3A)-C(28A)-F(2A)	107.9(5)
F(3A)-C(28A)-F(1A)	108.2(4)
F(2A)-C(28A)-F(1A)	107.5(4)
F(3A)-C(28A)-S(1A)	111.1(4)
F(2A)-C(28A)-S(1A)	110.8(4)
F(1A)-C(28A)-S(1A)	111.3(4)
O(1)-N(1)-Fe(1)	163.0(2)
C(1)-N(2)-C(5)	118.61(17)
C(1)-N(2)-Fe(1)	124.63(14)
C(5)-N(2)-Fe(1)	116.45(12)
C(7)-N(3)-C(6)	112.04(15)
C(7)-N(3)-C(13)	111.56(15)
C(6)-N(3)-C(13)	108.03(15)
C(7)-N(3)-Fe(1)	108.95(12)
C(6)-N(3)-Fe(1)	107.86(11)
C(13)-N(3)-Fe(1)	108.26(11)
C(12)-N(4)-C(8)	118.38(18)
C(12)-N(4)-Fe(1)	124.43(14)
C(8)-N(4)-Fe(1)	116.16(13)
N(2)-C(1)-C(2)	122.4(2)
N(2)-C(1)-H(1A)	118.8
C(2)-C(1)-H(1A)	118.8
C(1)-C(2)-C(3)	118.8(2)
C(1)-C(2)-H(2A)	120.6
C(3)-C(2)-H(2A)	120.6
C(2)-C(3)-C(4)	119.2(2)
C(2)-C(3)-H(3A)	120.4
C(4)-C(3)-H(3A)	120.4
C(3)-C(4)-C(5)	119.1(2)
C(3)-C(4)-H(4A)	120.4
C(5)-C(4)-H(4A)	120.4
N(2)-C(5)-C(4)	121.80(19)
N(2)-C(5)-C(6)	115.97(17)
C(4)-C(5)-C(6)	122.20(19)
N(3)-C(6)-C(5)	109.44(15)
N(3)-C(6)-H(6A)	109.8

SUPPORTING INFORMATION

C(5)-C(6)-H(6A)	109.8
N(3)-C(6)-H(6B)	109.8
C(5)-C(6)-H(6B)	109.8
H(6A)-C(6)-H(6B)	108.2
N(3)-C(7)-C(8)	110.51(16)
N(3)-C(7)-H(7A)	109.5
C(8)-C(7)-H(7A)	109.5
N(3)-C(7)-H(7B)	109.5
C(8)-C(7)-H(7B)	109.5
H(7A)-C(7)-H(7B)	108.1
N(4)-C(8)-C(9)	121.89(19)
N(4)-C(8)-C(7)	116.19(17)
C(9)-C(8)-C(7)	121.90(19)
C(10)-C(9)-C(8)	119.2(2)
C(10)-C(9)-H(9A)	120.4
C(8)-C(9)-H(9A)	120.4
C(9)-C(10)-C(11)	119.1(2)
C(9)-C(10)-H(10A)	120.5
C(11)-C(10)-H(10A)	120.5
C(10)-C(11)-C(12)	118.9(2)
C(10)-C(11)-H(11A)	120.5
C(12)-C(11)-H(11A)	120.5
N(4)-C(12)-C(11)	122.5(2)
N(4)-C(12)-H(12A)	118.7
C(11)-C(12)-H(12A)	118.7
N(3)-C(13)-C(14)	115.18(15)
N(3)-C(13)-H(13A)	108.5
C(14)-C(13)-H(13A)	108.5
N(3)-C(13)-H(13B)	108.5
C(14)-C(13)-H(13B)	108.5
H(13A)-C(13)-H(13B)	107.5
C(15)-C(14)-C(19)	120.89(17)
C(15)-C(14)-C(13)	120.65(16)
C(19)-C(14)-C(13)	118.34(16)
C(14)-C(15)-C(16)	121.59(17)
C(14)-C(15)-H(15A)	119.2
C(16)-C(15)-H(15A)	119.2
C(15)-C(16)-C(17)	116.82(16)
C(15)-C(16)-C(20)	120.73(16)
C(17)-C(16)-C(20)	122.36(17)
C(16)-C(17)-C(18)	123.95(17)
C(16)-C(17)-H(17A)	118.0
C(18)-C(17)-H(17A)	118.0
C(17)-C(18)-C(19)	117.72(16)
C(17)-C(18)-C(24)	121.22(16)
C(19)-C(18)-C(24)	120.99(15)
O(2)-C(19)-C(14)	119.25(16)
O(2)-C(19)-C(18)	121.90(16)
C(14)-C(19)-C(18)	118.84(16)
C(23)-C(20)-C(16)	112.28(15)
C(23)-C(20)-C(21)	107.78(17)
C(16)-C(20)-C(21)	110.88(16)
C(23)-C(20)-C(22)	108.76(17)
C(16)-C(20)-C(22)	107.69(16)
C(21)-C(20)-C(22)	109.40(17)
C(20)-C(21)-H(21A)	109.5
C(20)-C(21)-H(21B)	109.5

SUPPORTING INFORMATION

H(21A)-C(21)-H(21B)	109.5
C(20)-C(21)-H(21C)	109.5
H(21A)-C(21)-H(21C)	109.5
H(21B)-C(21)-H(21C)	109.5
C(20)-C(22)-H(22A)	109.5
C(20)-C(22)-H(22B)	109.5
H(22A)-C(22)-H(22B)	109.5
C(20)-C(22)-H(22C)	109.5
H(22A)-C(22)-H(22C)	109.5
H(22B)-C(22)-H(22C)	109.5
C(20)-C(23)-H(23A)	109.5
C(20)-C(23)-H(23B)	109.5
H(23A)-C(23)-H(23B)	109.5
C(20)-C(23)-H(23C)	109.5
H(23A)-C(23)-H(23C)	109.5
H(23B)-C(23)-H(23C)	109.5
C(27)-C(24)-C(18)	112.57(15)
C(27)-C(24)-C(26)	107.42(16)
C(18)-C(24)-C(26)	108.26(15)
C(27)-C(24)-C(25)	107.25(16)
C(18)-C(24)-C(25)	111.63(15)
C(26)-C(24)-C(25)	109.61(16)
C(24)-C(25)-H(25A)	109.5
C(24)-C(25)-H(25B)	109.5
H(25A)-C(25)-H(25B)	109.5
C(24)-C(25)-H(25C)	109.5
H(25A)-C(25)-H(25C)	109.5
H(25B)-C(25)-H(25C)	109.5
C(24)-C(26)-H(26A)	109.5
C(24)-C(26)-H(26B)	109.5
H(26A)-C(26)-H(26B)	109.5
C(24)-C(26)-H(26C)	109.5
H(26A)-C(26)-H(26C)	109.5
H(26B)-C(26)-H(26C)	109.5
C(24)-C(27)-H(27A)	109.5
C(24)-C(27)-H(27B)	109.5
H(27A)-C(27)-H(27B)	109.5
C(24)-C(27)-H(27C)	109.5
H(27A)-C(27)-H(27C)	109.5
H(27B)-C(27)-H(27C)	109.5

Symmetry transformations used to generate equivalent atoms:

SUPPORTING INFORMATION

Table S19. Anisotropic displacement parameters ($\text{\AA}^2 \times 10^3$) for complex **3**.

The anisotropic displacement factor exponent takes the form:

$$-2\pi^2 [h^2 a^{*2} U_{11} + \dots + 2 h k a^* b^* U_{12}]$$

	U11	U22	U33	U23	U13	U12
Fe(1)	21(1)	18(1)	24(1)	0(1)	8(1)	2(1)
O(1)	97(2)	50(1)	97(2)	28(1)	34(2)	-18(1)
O(2)	21(1)	15(1)	27(1)	1(1)	7(1)	2(1)
S(1)	21(1)	18(1)	23(1)	-1(1)	8(1)	0(1)
O(3)	24(2)	22(3)	29(2)	5(2)	5(1)	2(2)
O(4)	34(1)	24(1)	39(2)	4(1)	22(1)	2(1)
O(5)	30(2)	32(2)	38(2)	-14(1)	11(1)	-8(1)
C(28)	24(2)	28(2)	30(2)	4(1)	9(2)	4(1)
F(1)	36(1)	44(1)	40(2)	10(1)	9(1)	18(1)
F(2)	38(2)	21(1)	45(1)	-8(1)	16(1)	-1(1)
F(3)	31(2)	35(2)	43(2)	-2(1)	23(2)	-1(2)
S(1A)	23(1)	19(1)	22(1)	2(1)	9(1)	2(1)
O(3A)	24(3)	15(5)	25(4)	4(3)	6(2)	0(2)
O(4A)	38(3)	19(2)	29(2)	0(2)	4(2)	-1(2)
O(5A)	25(3)	41(3)	32(3)	8(2)	14(3)	8(3)
C(28A)	20(3)	24(3)	30(3)	2(2)	12(2)	2(2)
F(1A)	33(2)	31(2)	27(2)	0(1)	17(2)	-6(1)
F(2A)	33(2)	31(2)	38(2)	-9(2)	14(2)	-14(2)
F(3A)	36(2)	46(2)	32(2)	4(2)	4(2)	20(2)
N(1)	29(1)	25(1)	29(1)	2(1)	5(1)	4(1)
N(2)	22(1)	22(1)	27(1)	-2(1)	5(1)	4(1)
N(3)	21(1)	20(1)	25(1)	-5(1)	7(1)	-1(1)
N(4)	22(1)	29(1)	20(1)	0(1)	5(1)	5(1)
C(1)	33(1)	23(1)	37(1)	-3(1)	8(1)	4(1)
C(2)	49(2)	27(1)	45(1)	-10(1)	16(1)	6(1)
C(3)	42(1)	39(1)	38(1)	-10(1)	17(1)	10(1)
C(4)	27(1)	37(1)	28(1)	-4(1)	10(1)	7(1)
C(5)	19(1)	28(1)	26(1)	-3(1)	5(1)	4(1)
C(6)	18(1)	27(1)	28(1)	-3(1)	8(1)	0(1)
C(7)	27(1)	23(1)	34(1)	-10(1)	9(1)	-4(1)
C(8)	28(1)	27(1)	22(1)	-4(1)	5(1)	2(1)
C(9)	38(1)	27(1)	31(1)	-7(1)	9(1)	3(1)
C(10)	49(1)	35(1)	30(1)	-5(1)	13(1)	15(1)
C(11)	37(1)	48(1)	24(1)	3(1)	14(1)	17(1)
C(12)	27(1)	39(1)	20(1)	4(1)	9(1)	9(1)
C(13)	22(1)	21(1)	26(1)	1(1)	10(1)	-1(1)
C(14)	20(1)	20(1)	22(1)	-1(1)	8(1)	-1(1)
C(15)	24(1)	18(1)	24(1)	1(1)	9(1)	-3(1)
C(16)	25(1)	17(1)	22(1)	2(1)	9(1)	-1(1)
C(17)	19(1)	18(1)	24(1)	2(1)	7(1)	1(1)
C(18)	21(1)	16(1)	22(1)	1(1)	9(1)	-2(1)
C(19)	22(1)	15(1)	20(1)	-1(1)	8(1)	0(1)
C(20)	27(1)	15(1)	30(1)	4(1)	9(1)	-1(1)
C(21)	37(1)	25(1)	46(1)	14(1)	18(1)	2(1)
C(22)	36(1)	20(1)	39(1)	-2(1)	3(1)	2(1)
C(23)	28(1)	18(1)	33(1)	3(1)	7(1)	3(1)
C(24)	21(1)	16(1)	28(1)	3(1)	9(1)	0(1)
C(25)	23(1)	25(1)	34(1)	8(1)	11(1)	-2(1)
C(26)	27(1)	20(1)	36(1)	-3(1)	8(1)	-6(1)

SUPPORTING INFORMATION

C(27) 22(1) 24(1) 37(1) 7(1) 10(1) -1(1)

SUPPORTING INFORMATION

Table S20. Hydrogen coordinates ($x \times 10^4$) and isotropic displacement parameters ($\text{\AA}^2 \times 10^3$) for complex **3**.

	x	y	z	U(eq)
H(1A)	995	4402	7440	38
H(2A)	734	5413	8417	48
H(3A)	361	4198	8934	46
H(4A)	255	2000	8437	37
H(6A)	418	40	7683	29
H(6B)	316	610	6598	29
H(7A)	508	-930	5900	34
H(7B)	695	-1912	6760	34
H(9A)	953	-3250	5778	39
H(10A)	1366	-3392	5074	45
H(11A)	1630	-1458	4855	43
H(12A)	1475	548	5337	34
H(13A)	904	-1130	8316	27
H(13B)	1026	356	8540	27
H(15A)	1306	-2703	8485	26
H(17A)	2197	-1693	8442	24
H(21A)	1822	-5414	9555	52
H(21B)	1506	-4498	9190	52
H(21C)	1821	-3993	10031	52
H(22A)	1833	-4292	7226	51
H(22B)	1501	-4525	7453	51
H(22C)	1788	-5579	7806	51
H(23A)	2333	-3737	8518	41
H(23B)	2301	-4970	9167	41
H(23C)	2337	-3513	9611	41
H(25A)	2188	2244	7030	40
H(25B)	1814	1948	6890	40
H(25C)	2027	891	6542	40
H(26A)	2214	1531	9462	43
H(26B)	1932	2353	8698	43
H(26C)	2304	2625	8799	43
H(27A)	2543	-79	8883	41
H(27B)	2621	1050	8221	41
H(27C)	2469	-322	7746	41

SUPPORTING INFORMATION

Table S21. Torsion angles [deg] for complex 3.

O(5)-S(1)-O(3)-Fe(1)	143.1(7)
O(4)-S(1)-O(3)-Fe(1)	5.9(10)
C(28)-S(1)-O(3)-Fe(1)	-105.5(9)
O(5)-S(1)-C(28)-F(1)	-61.1(3)
O(4)-S(1)-C(28)-F(1)	62.2(3)
O(3)-S(1)-C(28)-F(1)	-178.7(3)
O(5)-S(1)-C(28)-F(2)	179.1(2)
O(4)-S(1)-C(28)-F(2)	-57.7(3)
O(3)-S(1)-C(28)-F(2)	61.4(3)
O(5)-S(1)-C(28)-F(3)	59.4(3)
O(4)-S(1)-C(28)-F(3)	-177.4(3)
O(3)-S(1)-C(28)-F(3)	-58.3(4)
O(5A)-S(1A)-O(3A)-Fe(1)	-96.9(9)
O(4A)-S(1A)-O(3A)-Fe(1)	39.1(12)
C(28A)-S(1A)-O(3A)-Fe(1)	151.3(8)
O(5A)-S(1A)-C(28A)-F(3A)	62.8(5)
O(4A)-S(1A)-C(28A)-F(3A)	-59.8(5)
O(3A)-S(1A)-C(28A)-F(3A)	-177.9(5)
O(5A)-S(1A)-C(28A)-F(2A)	-57.1(5)
O(4A)-S(1A)-C(28A)-F(2A)	-179.7(4)
O(3A)-S(1A)-C(28A)-F(2A)	62.3(5)
O(5A)-S(1A)-C(28A)-F(1A)	-176.6(5)
O(4A)-S(1A)-C(28A)-F(1A)	60.7(4)
O(3A)-S(1A)-C(28A)-F(1A)	-57.3(5)
O(2)-Fe(1)-N(1)-O(1)	-127.5(7)
N(2)-Fe(1)-N(1)-O(1)	-30.1(7)
N(4)-Fe(1)-N(1)-O(1)	137.8(7)
N(3)-Fe(1)-N(1)-O(1)	34.3(9)
O(3)-Fe(1)-N(1)-O(1)	54.9(8)
O(3A)-Fe(1)-N(1)-O(1)	53.5(8)
C(5)-N(2)-C(1)-C(2)	-0.4(3)
Fe(1)-N(2)-C(1)-C(2)	-173.76(17)
N(2)-C(1)-C(2)-C(3)	1.1(4)
C(1)-C(2)-C(3)-C(4)	-0.4(4)
C(2)-C(3)-C(4)-C(5)	-0.8(3)
C(1)-N(2)-C(5)-C(4)	-1.0(3)
Fe(1)-N(2)-C(5)-C(4)	172.95(15)
C(1)-N(2)-C(5)-C(6)	177.43(17)
Fe(1)-N(2)-C(5)-C(6)	-8.6(2)
C(3)-C(4)-C(5)-N(2)	1.6(3)
C(3)-C(4)-C(5)-C(6)	-176.74(19)
C(7)-N(3)-C(6)-C(5)	-159.46(16)
C(13)-N(3)-C(6)-C(5)	77.26(19)
Fe(1)-N(3)-C(6)-C(5)	-39.55(17)
N(2)-C(5)-C(6)-N(3)	33.2(2)
C(4)-C(5)-C(6)-N(3)	-148.40(18)
C(6)-N(3)-C(7)-C(8)	154.83(17)
C(13)-N(3)-C(7)-C(8)	-83.9(2)
Fe(1)-N(3)-C(7)-C(8)	35.56(19)
C(12)-N(4)-C(8)-C(9)	-0.6(3)
Fe(1)-N(4)-C(8)-C(9)	-169.51(16)
C(12)-N(4)-C(8)-C(7)	-178.93(17)
Fe(1)-N(4)-C(8)-C(7)	12.2(2)

SUPPORTING INFORMATION

N(3)-C(7)-C(8)-N(4)	-32.7(2)
N(3)-C(7)-C(8)-C(9)	149.03(19)
N(4)-C(8)-C(9)-C(10)	0.8(3)
C(7)-C(8)-C(9)-C(10)	179.1(2)
C(8)-C(9)-C(10)-C(11)	-0.4(3)
C(9)-C(10)-C(11)-C(12)	-0.1(3)
C(8)-N(4)-C(12)-C(11)	0.0(3)
Fe(1)-N(4)-C(12)-C(11)	167.90(15)
C(10)-C(11)-C(12)-N(4)	0.4(3)
C(7)-N(3)-C(13)-C(14)	65.5(2)
C(6)-N(3)-C(13)-C(14)	-170.98(15)
Fe(1)-N(3)-C(13)-C(14)	-54.42(17)
N(3)-C(13)-C(14)-C(15)	-117.29(19)
N(3)-C(13)-C(14)-C(19)	66.7(2)
C(19)-C(14)-C(15)-C(16)	0.4(3)
C(13)-C(14)-C(15)-C(16)	-175.48(18)
C(14)-C(15)-C(16)-C(17)	2.6(3)
C(14)-C(15)-C(16)-C(20)	-173.89(17)
C(15)-C(16)-C(17)-C(18)	-2.2(3)
C(20)-C(16)-C(17)-C(18)	174.30(18)
C(16)-C(17)-C(18)-C(19)	-1.4(3)
C(16)-C(17)-C(18)-C(24)	175.64(18)
Fe(1)-O(2)-C(19)-C(14)	-49.8(2)
Fe(1)-O(2)-C(19)-C(18)	130.40(15)
C(15)-C(14)-C(19)-O(2)	176.07(16)
C(13)-C(14)-C(19)-O(2)	-7.9(3)
C(15)-C(14)-C(19)-C(18)	-4.1(3)
C(13)-C(14)-C(19)-C(18)	171.92(16)
C(17)-C(18)-C(19)-O(2)	-175.71(17)
C(24)-C(18)-C(19)-O(2)	7.3(3)
C(17)-C(18)-C(19)-C(14)	4.5(3)
C(24)-C(18)-C(19)-C(14)	-172.56(17)
C(15)-C(16)-C(20)-C(23)	-164.67(18)
C(17)-C(16)-C(20)-C(23)	19.0(3)
C(15)-C(16)-C(20)-C(21)	-44.0(2)
C(17)-C(16)-C(20)-C(21)	139.62(19)
C(15)-C(16)-C(20)-C(22)	75.6(2)
C(17)-C(16)-C(20)-C(22)	-100.7(2)
C(17)-C(18)-C(24)-C(27)	2.5(3)
C(19)-C(18)-C(24)-C(27)	179.46(17)
C(17)-C(18)-C(24)-C(26)	-116.05(19)
C(19)-C(18)-C(24)-C(26)	60.9(2)
C(17)-C(18)-C(24)-C(25)	123.22(19)
C(19)-C(18)-C(24)-C(25)	-59.9(2)

Symmetry transformations used to generate equivalent atoms:

SUPPORTING INFORMATION

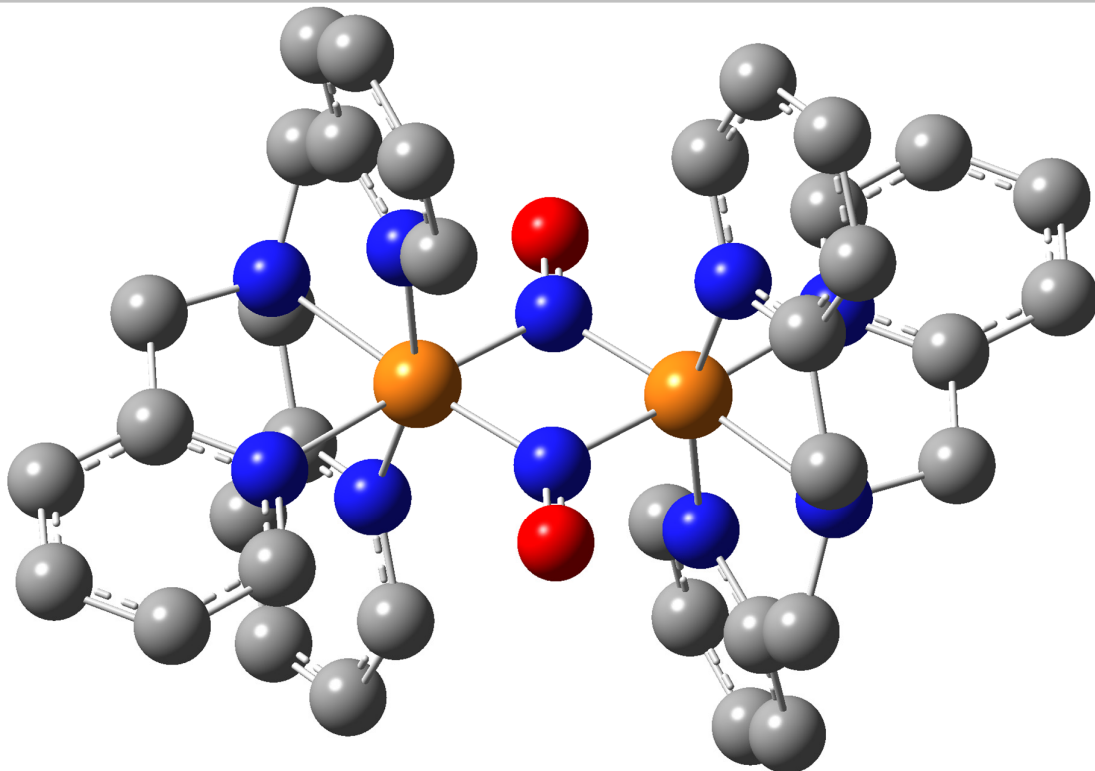


Figure S27. Optimized structure of complex **2** using BP86/TZVP. Hydrogen atoms are omitted for clarity.

Table S22. Comparison of important values between experimental data and DFT calculated data of complex **2** showing a high degree of agreement.

Parameters	Experimental Data	DFT
N–O	1.247 Å	1.248 Å
Fe1–N	1.820 Å	1.825 Å
Fe1A–N1	1.876 Å	1.885 Å
Fe–Fe	2.895 Å	2.920 Å
Fe1–N1–Fe1A	103.1 deg.	103.9 deg.
$\nu_{\text{antisymm}}(\text{N–O})$	1350 cm ⁻¹	1364 cm ⁻¹
$\nu_{\text{antisymm}}(^{15}\text{N–O})$	1330 cm ⁻¹	1333 cm ⁻¹
$\nu_{\text{antisymm}}(^{15}\text{N–}^{18}\text{O})$	1306 cm ⁻¹	1309 cm ⁻¹
δ	0.31 mm/s	0.28 mm/s
$ \Delta E_Q $	1.40 mm/s	1.66 mm/s

SUPPORTING INFORMATION

Table S23. DFT optimized coordinates of complex **2**, obtained with BP86/TZVP.

Fe	-1.44859100	0.10562400	0.15288600
N	-0.15731300	0.00749100	-1.13328700
O	-0.28237300	0.07950000	-2.37281700
Fe	1.44859600	-0.10565700	-0.15286600
N	0.15731900	-0.00752800	1.13331200
O	0.28238300	-0.07951800	2.37284300
N	-2.81887500	0.27418600	1.74973600
N	-1.87838500	-1.83287600	0.39401100
N	-3.19859200	0.14630900	-0.97930400
N	-1.59203700	2.09485000	0.26806400
N	2.81885400	-0.27423500	-1.74972900
N	1.59206300	-2.09488400	-0.26801100
N	3.19861600	-0.14627200	0.97930700
N	1.87835700	1.83284600	-0.39403500
C	-3.29514900	0.01362800	-2.32484200
C	-4.51772800	-0.05146800	-2.98917300
C	-2.86348300	-4.41411500	0.84638400
C	-2.11715800	4.82281100	0.59134300
C	-2.37818400	1.49889400	2.47637300
C	-2.36978200	3.92161800	1.63172600
C	-2.10466300	2.56570300	1.44231400
C	-2.21823200	-4.09659400	-0.35104800
C	-3.02134300	-3.41265600	1.80954500
C	-1.61854400	4.33103400	-0.61691600
C	-2.64922900	-0.98362000	2.52674900
H	-2.09094700	-4.83807000	-1.14044700
H	-0.99111600	2.53241300	-1.66882300
H	-2.34158900	-0.03062900	-2.85366300
H	-1.24320400	-2.50520100	-1.46373200
H	-6.67300500	-0.04444400	-2.73168200
H	-6.50548000	0.20313200	-0.24241600
H	-1.43123400	4.99181700	-1.46397600
H	-4.53663700	-0.15405500	-4.07477100
H	-1.44975900	1.24475100	3.01023300
H	-3.53819100	-3.61519900	2.74930200
H	-1.71079400	-0.88862800	3.09459200
H	-3.12559700	1.84004000	3.21336100
H	-3.47649100	-1.14848900	3.23845600
H	-3.25293400	-5.41807900	1.02290800
H	-4.56192800	1.45424500	1.46381500
H	-4.89662000	-0.24727600	1.77142300
H	-2.32780500	5.88610200	0.71744800
H	-2.78582200	4.26357500	2.58116600
C	-5.60592300	0.14731800	-0.85889600
C	-2.52587200	-2.13341300	1.55652100
C	-1.36898300	2.96493700	-0.74151000
C	-4.34399300	0.21730500	-0.25919500
C	-1.74192300	-2.80052400	-0.54049600
C	-5.69819200	0.01101700	-2.24407300
C	-4.21782600	0.43319300	1.23217100
C	4.34400400	-0.21725600	0.25917500
C	5.69824300	-0.01080000	2.24400700
C	5.60594600	-0.14717800	0.85883900
C	4.21780900	-0.43324500	-1.23217400

SUPPORTING INFORMATION

C	1.36904700	-2.96495900	0.74158100
C	2.52583700	2.13336800	-1.55655100
C	1.74186700	2.80051600	0.54044500
C	3.29520200	-0.01351400	2.32483500
C	4.51779600	0.05167100	2.98913200
C	2.86339300	4.41409600	-0.84647400
C	2.11720200	-4.82284500	-0.59126800
C	2.37815300	-1.49895100	-2.47634600
C	2.36978500	-3.92166400	-1.63167100
C	2.10466200	-2.56574800	-1.44226900
C	2.21814100	4.09659200	0.35096300
C	3.02127900	3.41261600	-1.80960800
C	1.61862100	-4.33105600	0.61700000
C	2.64919800	0.98355800	-2.52675900
H	2.09082800	4.83808900	1.14033800
H	0.99121000	-2.53242600	1.66890100
H	2.34165400	0.03072700	2.85367900
H	1.24314300	2.50520600	1.46368400
H	6.67306600	0.04473100	2.73158800
H	6.50549000	-0.20298200	0.24234000
H	1.43134800	-4.99182800	1.46407600
H	4.53672700	0.15431600	4.07472400
H	1.44971700	-1.24481500	-3.01019100
H	3.53811800	3.61514800	-2.74937200
H	1.71076000	0.88855400	-3.09459500
H	3.12555400	-1.84009900	-3.21334600
H	3.47645500	1.14842200	-3.23847300
H	3.25281400	5.41806700	-1.02302600
H	4.56187100	-1.45432800	-1.46374200
H	4.89662100	0.24715700	-1.77148700
H	2.32785900	-5.88613600	-0.71736300
H	2.78580300	-4.26363000	-2.58111800

SUPPORTING INFORMATION

Table S24. DFT optimized coordinates of complex **2**, obtained with B3LYP/TZVP.

Fe	-1.48887400	0.00212400	0.15270100
N	-3.23732600	0.00269900	-1.00294600
N	-1.77142700	2.00310700	0.33661300
O	-0.26651600	0.00033700	-2.36577200
N	-1.77692600	-1.99785200	0.33911800
N	-0.13883800	-0.00016600	-1.14225900
N	-2.87667400	0.00523300	1.73392700
C	-4.37771300	0.00352300	-0.29576900
C	-5.70459700	-0.00093600	-2.29172100
C	-5.62793200	0.00158700	-0.90750300
C	-4.27661000	0.00799100	1.21190500
C	-1.58173600	2.93191900	-0.61115200
C	-2.36806400	-2.35892000	1.50011100
C	-1.58921200	-2.92843600	-0.60734300
C	-3.31609100	0.00029500	-2.34678500
C	-4.52339300	-0.00143100	-3.02460000
C	-2.54134100	-4.63488200	0.76714900
C	-2.52798500	4.64282800	0.76185200
C	-2.57530200	1.24797200	2.48669800
C	-2.74360200	3.67900400	1.74052400
C	-2.36069600	2.36731600	1.49762800
C	-1.95531800	-4.25420400	-0.43282800
C	-2.75486200	-3.66922300	1.74443200
C	-1.94393000	4.25897400	-0.43804200
C	-2.57993400	-1.23787000	2.48782500
H	-1.79103500	-4.96647200	-1.22980000
H	-1.13532700	2.58783600	-1.53396900
H	-2.36770100	-0.00016500	-2.86610600
H	-1.14111300	-2.58685100	-1.53026000
H	-6.66635000	-0.00245700	-2.78850600
H	-6.52674200	0.00216800	-0.30348400
H	-1.77808200	4.96973400	-1.23603600
H	-4.53230600	-0.00325800	-4.10605900
H	-1.65587300	1.07763100	3.04713200
H	-3.23121400	-3.92464800	2.68210000
H	-1.66034600	-1.07005300	3.04878000
H	-3.36839400	1.50132500	3.19641600
H	-3.37436100	-1.48803600	3.19718600
H	-2.84447600	-5.66045700	0.93448700
H	-4.80338100	0.88323700	1.59872500
H	-4.80977900	-0.86053600	1.60509400
H	-2.82812500	5.66946400	0.92809500
H	-3.21864200	3.93699300	2.67816100
Fe	1.48887300	-0.00206300	-0.15272700
N	3.23729500	-0.00271200	1.00295600
N	1.77145200	-2.00304600	-0.33662400
O	0.26651200	-0.00028200	2.36574100
N	1.77690600	1.99791400	-0.33914700
N	0.13883500	0.00022100	1.14223000
N	2.87670600	-0.00513600	-1.73392500
C	4.37769800	-0.00364700	0.29580500
C	5.70453200	0.00036600	2.29179100
C	5.62790200	-0.00200400	0.90757000
C	4.27662900	-0.00778900	-1.21187300

SUPPORTING INFORMATION

C	1.58174600	-2.93185600	0.61114100
C	2.36800900	2.35899500	-1.50015600
C	1.58918300	2.92849500	0.60731400
C	3.31602500	-0.00045900	2.34679700
C	4.52331000	0.00100400	3.02464300
C	2.54121600	4.63496800	-0.76720800
C	2.52813900	-4.64274300	-0.76179000
C	2.57542500	-1.24790700	-2.48667500
C	2.74377300	-3.67892100	-1.74046100
C	2.36080100	-2.36724600	-1.49760200
C	1.95523300	4.25427600	0.43278400
C	2.75475500	3.66931100	-1.74449000
C	1.94399900	-4.25889900	0.43806500
C	2.57992700	1.23794000	-2.48785500
H	1.79094100	4.96654300	1.22975500
H	1.13527700	-2.58778000	1.53393100
H	2.36762100	0.00009800	2.86609400
H	1.14111200	2.58689800	1.53024200
H	6.66627200	0.00166500	2.78860000
H	6.52672600	-0.00268000	0.30357400
H	1.77813500	-4.96965600	1.23605800
H	4.53219700	0.00273000	4.10610200
H	1.65602000	-1.07761200	-3.04716300
H	3.23108100	3.92474800	-2.68216700
H	1.66035200	1.07007600	-3.04881700
H	3.36856500	-1.50124200	-3.19634800
H	3.37435200	1.48812400	-3.19721100
H	2.84430900	5.66055400	-0.93455900
H	4.80358700	-0.88282300	-1.59891700
H	4.80962900	0.86095300	-1.60481700
H	2.82833300	-5.66936800	-0.92800400
H	3.21888300	-3.93690000	-2.67806500

Table S25. Comparison of important experimental and DFT-calculated parameters for complex **2**, showing an overestimation in the N–O stretching frequency when using the hybrid functional B3LYP.

Parameters	Experimental Data	DFT (B3LYP/TZVP)
N–O	1.247 Å	1.23 Å
Fe1–N	1.820 Å	1.87 Å
Fe1A–N1	1.876 Å	1.90 Å
Fe–Fe	2.895 Å	2.993 Å
Fe1–N1–Fe1A	103.1 deg.	104.9 deg.
$\nu_{\text{antisymm}}(\text{N–O})$	1350 cm ⁻¹	1452 cm ⁻¹

SUPPORTING INFORMATION

Table S26. DFT optimized coordinates of high-spin complex **1** with triflate counter anion bound, obtained with B3LYP*/TZVP.

Fe	-0.35456800	0.07738700	0.56518400
S	2.83581600	0.15599000	0.11604100
F	3.84700500	-1.99815600	-1.10061300
F	3.50236000	-2.26335300	1.03279700
F	5.18776300	-1.06999200	0.34211300
N	-0.01160500	0.04189100	2.32330400
N	0.05998200	2.17474600	0.07953100
N	-0.94747800	0.28886000	-1.64223900
N	-2.55332300	0.46536600	0.66438400
N	-0.99879200	-1.95656900	0.02410600
O	0.31330600	0.07417900	3.43110300
O	1.45003900	-0.48054300	-0.20384300
O	3.28967900	0.99711200	-1.00685400
O	2.87968500	0.68674700	1.49225500
C	0.29901300	3.14668600	0.97561500
H	0.22380300	2.87227400	2.02131500
C	0.64318600	4.43518700	0.60080100
H	0.83770600	5.18442900	1.35837500
C	0.73966100	4.72996500	-0.75482900
H	1.00908700	5.72728700	-1.08448000
C	0.49172700	3.72663300	-1.68376100
H	0.56848500	3.92150800	-2.74749000
C	0.16526100	2.45225800	-1.23499200
C	-0.00107800	1.29205800	-2.18659200
H	-0.31207900	1.64783700	-3.17657600
H	0.97702700	0.81590500	-2.29133900
C	-2.34826300	0.75787800	-1.75626200
H	-2.84436200	0.28678600	-2.61297400
H	-2.33034100	1.83245500	-1.96625600
C	-3.18939100	0.57185100	-0.51211800
C	-4.58035300	0.60246900	-0.58879000
H	-5.06796800	0.67943500	-1.55460300
C	-5.32702600	0.54063100	0.58013300
H	-6.41053200	0.56503500	0.54124700
C	-4.66310100	0.44770500	1.80000500
H	-5.20426500	0.40092800	2.73726500
C	-3.27858700	0.40504800	1.79470300
H	-2.72147700	0.31863800	2.72120500
C	-0.73656900	-1.05443600	-2.22409100
H	0.33749700	-1.16964800	-2.39173300
H	-1.24090500	-1.15593900	-3.19323300
C	-1.15754200	-2.16979800	-1.29468200
C	-1.59431600	-3.39708500	-1.78356100
H	-1.71982600	-3.54050000	-2.85102100
C	-1.85109200	-4.43142000	-0.89128000
H	-2.18561700	-5.39737200	-1.25335000
C	-1.66791600	-4.21019400	0.46953200
H	-1.84843400	-4.99011900	1.19926100
C	-1.24691500	-2.95597100	0.88440800
H	-1.09438500	-2.73865400	1.93594700
C	3.92579700	-1.40691400	0.09633400

SUPPORTING INFORMATION

Table S27. DFT optimized coordinates of low-spin complex **1** with triflate counter anion bound, obtained with B3LYP*/TZVP.

Fe	0.47932200	0.14106700	0.40589700
S	-2.50999900	-0.90561800	0.01467300
F	-4.18794100	0.98687300	-0.85090900
F	-4.05740400	0.84424300	1.31768000
F	-5.14895700	-0.66526600	0.19191900
N	0.12498900	0.13718700	2.13711100
N	0.57322800	-1.84629200	0.09830200
N	0.90028400	0.20491000	-1.65307900
N	2.48399900	0.12608700	0.57678900
N	0.40754800	2.13933100	0.12499900
O	-0.68980800	0.47972200	2.89309700
O	-1.46400300	0.24762800	-0.01464700
O	-2.59788300	-1.56893200	-1.30568300
O	-2.41019600	-1.73662800	1.22773300
C	0.61690700	-2.79851100	1.04561300
H	0.53065200	-2.46194600	2.07077400
C	0.73958800	-4.14280800	0.73660900
H	0.75519100	-4.87621000	1.53333600
C	0.82916800	-4.51861800	-0.59881300
H	0.92492200	-5.56307200	-0.87365200
C	0.78380800	-3.53539500	-1.57954100
H	0.83471200	-3.79382100	-2.63106000
C	0.64399300	-2.20635500	-1.20214500
C	0.44263900	-1.09967500	-2.20361400
H	0.93684000	-1.32782100	-3.15414000
H	-0.63485500	-1.03553400	-2.38592900
C	2.36285700	0.42829200	-1.83321600
H	2.51944400	1.47477500	-2.11308200
H	2.74227300	-0.17519400	-2.66409800
C	3.16476300	0.16388200	-0.58336100
C	4.54977200	0.03642900	-0.62038000
H	5.06867800	0.06305100	-1.57234700
C	5.25033400	-0.12091100	0.56808000
H	6.32998900	-0.22051300	0.56059700
C	4.54223700	-0.15029500	1.76565300
H	5.04506500	-0.27234300	2.71732800
C	3.16304400	-0.03264600	1.72764900
H	2.56542000	-0.06962900	2.63073100
C	0.11402500	1.36308400	-2.15396500
H	-0.93093100	1.05391100	-2.21118700
H	0.44020300	1.67526600	-3.15272200
C	0.21918000	2.49711800	-1.16577800
C	0.08800900	3.82873400	-1.53770300
H	-0.05625100	4.08390500	-2.58150400
C	0.13415900	4.81685200	-0.56060200
H	0.02442100	5.86129900	-0.83018500
C	0.32568300	4.44275400	0.76398200
H	0.36865500	5.17708300	1.55904100
C	0.46217000	3.09627400	1.06510200
H	0.61008300	2.76851400	2.08639500
C	-4.09290300	0.14261200	0.18352300

SUPPORTING INFORMATION

Table S28. DFT optimized coordinates of high-spin complex **1** with CH₃CN bound, obtained with B3LYP*/TZVP.

Fe	-0.00032100	-0.36840500	0.61126700
O	-0.00060200	-0.90193100	3.50947000
N	2.11801300	-0.38398100	0.10299500
N	0.00109700	1.79068200	0.56852100
N	-0.00043000	-0.64398900	2.38594700
C	-1.23351700	-0.62320300	-2.14686200
H	-1.04741600	-1.69904600	-2.20990000
C	3.12686500	-0.27571900	0.98634300
H	2.85675900	-0.26008700	2.03636100
C	0.00182300	2.57431100	1.66816000
H	0.00141400	2.06704200	2.62594100
N	-0.00018100	0.02001500	-1.62883600
H	-1.47569100	-0.27876100	-3.15857800
C	1.23248300	-0.62443100	-2.14692800
H	1.04526800	-1.70007900	-2.21002900
H	1.47497800	-0.28018000	-3.15863300
C	2.40168700	-0.40594000	-1.21598500
C	3.70726300	-0.30815000	-1.68136900
H	3.90604800	-0.31982300	-2.74733900
C	4.74886500	-0.20030000	-0.76475600
H	5.77506200	-0.12500400	-1.10740300
C	4.45362200	-0.18840000	0.59454900
H	5.23385400	-0.10615800	1.34168700
C	0.00050100	1.49157400	-1.87853800
H	0.87358900	1.75264100	-2.48482400
H	-0.87297900	1.75354500	-2.48387000
C	0.00155400	2.36906900	-0.64328000
C	0.00279300	3.75520100	-0.78720100
H	0.00315600	4.19702200	-1.77806600
C	0.00352900	4.55820800	0.34436700
H	0.00447900	5.63862400	0.25058600
C	0.00301800	3.95474400	1.60049700
H	0.00355000	4.54236000	2.51060500
C	-2.40244200	-0.40342100	-1.21587300
C	-3.70794300	-0.30432800	-1.68118800
C	-3.12735200	-0.27217200	0.98648500
C	-4.74937800	-0.19529000	-0.76452600
H	-3.90680600	-0.31591900	-2.74714500
C	-4.45404100	-0.18352200	0.59475900
H	-2.85716600	-0.25668800	2.03648500
H	-5.77551600	-0.11897400	-1.10712100
H	-5.23414100	-0.10037500	1.34193400
N	-2.11866400	-0.38159500	0.10309000
N	-0.00152400	-2.60655300	0.22923400
C	-0.00211900	-3.75665700	0.31044400
C	-0.00290300	-5.20118900	0.41283200
H	-0.89378200	-5.61053200	-0.07112700
H	0.88719100	-5.61153400	-0.07172200
H	-0.00271900	-5.49846800	1.46523500

SUPPORTING INFORMATION

Table S29. DFT optimized coordinates of low-spin complex **1** with CH₃CN bound, obtained with B3LYP*/TZVP.

Fe	-0.00003300	-0.34477700	0.41915300
O	-0.00056100	-1.39617500	3.01138400
N	1.99725600	-0.31518000	0.13248500
N	0.00017700	1.65996000	0.51668700
N	-0.00008200	-0.57279900	2.19011200
C	-1.24539700	-0.66766100	-2.13991100
H	-1.06236200	-1.74336400	-2.20370100
C	2.94693300	-0.14984400	1.07061100
H	2.61014700	-0.06127300	2.09625200
C	0.00027900	2.38565000	1.65319600
H	0.00023300	1.82582600	2.58021500
N	0.00001200	-0.02093900	-1.63713000
H	-1.50386500	-0.32061800	-3.14552500
C	1.24533500	-0.66785100	-2.13988400
H	1.06213200	-1.74352500	-2.20369100
H	1.50388200	-0.32083900	-3.14548900
C	2.36857600	-0.42084700	-1.16536400
C	3.70104500	-0.35792700	-1.54856000
H	3.96724500	-0.43546800	-2.59686800
C	4.68199000	-0.19685200	-0.57459500
H	5.72891800	-0.14856200	-0.85284400
C	4.29668800	-0.09452200	0.75702400
H	5.02570400	0.03447100	1.54800700
C	0.00012100	1.45536200	-1.91359100
H	0.87489100	1.70695900	-2.51991500
H	-0.87467100	1.70709700	-2.51982600
C	0.00024600	2.30147500	-0.66547300
C	0.00041400	3.69074800	-0.74295500
H	0.00046700	4.17877600	-1.71171400
C	0.00051000	4.43699500	0.42750900
H	0.00063800	5.52061400	0.38851500
C	0.00044200	3.76920000	1.64917000
H	0.00051700	4.30892700	2.58850000
C	-2.36861900	-0.42046300	-1.16541800
C	-3.70106700	-0.35733800	-1.54864700
C	-2.94698600	-0.14930900	1.07053400
C	-4.68201200	-0.19608100	-0.57471100
H	-3.96725500	-0.43486000	-2.59696000
C	-4.29672500	-0.09377800	0.75691400
H	-2.61022300	-0.06076800	2.09618500
H	-5.72892500	-0.14762800	-0.85298800
H	-5.02573800	0.03535400	1.54787700
N	-1.99731000	-0.31482400	0.13243800
N	-0.00022400	-2.32261300	0.24324900
C	-0.00034200	-3.47090200	0.33437200
C	-0.00041400	-4.91371900	0.45783900
H	-0.89144800	-5.33326900	-0.01703900
H	0.89028500	-5.33341200	-0.01754000
H	-0.00013800	-5.19007600	1.51625800

SUPPORTING INFORMATION

Table S30. DFT optimized coordinates of the low-spin {FeNO}⁸ complex **1red** with triflate bound, obtained with B3LYP*/TZVP.

Fe	0.52707300	0.16495700	0.49567400
S	-2.52062100	-0.96231500	-0.16802800
F	-4.26120300	1.07769900	-0.33748300
F	-4.19933100	0.13222400	1.62216900
F	-5.18550800	-0.87027900	-0.03758600
N	0.43473700	0.06575200	2.26754300
N	0.71384500	-1.81202600	0.17633200
N	0.89194500	0.22552700	-1.69808300
N	2.52515300	0.25788300	0.51152700
N	0.25620300	2.13079600	0.15497700
O	-0.31760200	0.77258400	2.90538900
O	-1.52293700	0.11397700	0.23896000
O	-2.60228800	-1.11228000	-1.64963800
O	-2.47821200	-2.20112100	0.63388700
C	0.80645300	-2.74163300	1.14032800
H	0.72163300	-2.36043200	2.15288700
C	0.99112500	-4.08623600	0.86050500
H	1.04620400	-4.80138300	1.67269600
C	1.09601700	-4.48619600	-0.46699200
H	1.24195300	-5.53031900	-0.72221900
C	1.00512200	-3.52402100	-1.46531200
H	1.07271100	-3.79900800	-2.51239100
C	0.80319500	-2.19293700	-1.11565600
C	0.56031800	-1.13040100	-2.16975500
H	1.10716400	-1.38446000	-3.08881000
H	-0.50980000	-1.15593400	-2.40150700
C	2.30157300	0.59852600	-1.89170200
H	2.34595600	1.67033500	-2.11279300
H	2.73190800	0.08433300	-2.76183900
C	3.16187600	0.35043700	-0.67351600
C	4.54856900	0.28534300	-0.77070700
H	5.02028300	0.35208100	-1.74562100
C	5.30989000	0.13383800	0.38104300
H	6.39188200	0.08264700	0.32561100
C	4.65023000	0.04036100	1.60278500
H	5.19505200	-0.08748300	2.53097900
C	3.26606000	0.09486900	1.62534000
H	2.69028300	-0.00878400	2.54035200
C	-0.03637000	1.28911900	-2.12159500
H	-1.04451500	0.86776500	-2.12888300
H	0.18336900	1.65785000	-3.13456200
C	-0.00655300	2.43829300	-1.13582800
C	-0.27999700	3.74302500	-1.53159000
H	-0.48327000	3.95448800	-2.57582500
C	-0.30194000	4.75632000	-0.57957700
H	-0.52129100	5.77841800	-0.86915800
C	-0.04148800	4.43189900	0.74602100
H	-0.05466400	5.18429900	1.52567700
C	0.23227900	3.11020600	1.07177100
H	0.40100500	2.79737400	2.09455100
C	-4.14641300	-0.09601700	0.30660800

SUPPORTING INFORMATION

Table S31. DFT optimized coordinates of the high-spin {FeNO}⁸ complex **1red** with triflate bound, obtained with B3LYP*/TZVP.

Fe	-0.47613000	0.18064000	0.73083800
S	2.93538100	0.04428600	-0.06361400
F	3.70370000	-2.48899100	-0.54299800
F	3.87051500	-1.89837500	1.54536100
F	5.31958300	-1.17542600	0.09174600
N	-0.52290900	0.15400000	2.52394000
N	0.12992800	2.21717800	0.18246700
N	-0.80227600	0.35350000	-1.62627700
N	-2.68143900	0.52587500	0.48885300
N	-0.98606100	-1.86033900	0.09160500
O	-0.99298800	0.22444700	3.62310400
O	1.55050500	-0.53628600	0.16563700
O	3.18154800	0.34782600	-1.50177100
O	3.35771500	1.05655800	0.92657800
C	0.35268900	3.17842100	1.09163400
H	0.21374000	2.89190400	2.12817500
C	0.75027100	4.46114500	0.74633400
H	0.92723500	5.19865300	1.52017000
C	0.92064000	4.76548900	-0.59992800
H	1.23070800	5.75788500	-0.90916000
C	0.69466300	3.77191100	-1.54417500
H	0.82992000	3.96697000	-2.60261800
C	0.31191300	2.50280200	-1.11888800
C	0.17477500	1.35565200	-2.09427100
H	-0.08220000	1.73876800	-3.09254200
H	1.15832700	0.88022400	-2.16934300
C	-2.18362200	0.79622100	-1.88170700
H	-2.56337600	0.37622900	-2.82406400
H	-2.16293800	1.88334300	-2.01364400
C	-3.16554600	0.52043000	-0.76466300
C	-4.52455100	0.37480800	-1.03246000
H	-4.87323100	0.35917800	-2.05990400
C	-5.41851400	0.25725400	0.02537100
H	-6.48118800	0.14374200	-0.15997900
C	-4.91936600	0.28982900	1.32354200
H	-5.57389900	0.20782400	2.18354500
C	-3.54960900	0.41516500	1.50848500
H	-3.12000300	0.42535500	2.50488700
C	-0.51509300	-0.99882900	-2.13391000
H	0.57260200	-1.10406900	-2.16928500
H	-0.90208700	-1.14081800	-3.15414400
C	-1.02822100	-2.09768200	-1.23022400
C	-1.42818800	-3.33001700	-1.74121000
H	-1.45787000	-3.48504300	-2.81454500
C	-1.77168800	-4.35107100	-0.86314000
H	-2.07941800	-5.32069900	-1.23966600
C	-1.70812000	-4.10673100	0.50497100
H	-1.95846800	-4.87338200	1.22884500
C	-1.31743700	-2.84690100	0.93656800
H	-1.25744200	-2.60654700	1.99297300
C	4.02729500	-1.47647000	0.28214700

SUPPORTING INFORMATION

References

1. CrystalClear Expert, 2.0 r16, C. E. Rigaku Americas: 9009, TX, USA; Rigaku Tokyo, 196-8666, Japan, 2014.
2. Sheldrick, G. Crystal structure refinement with SHELXL. *Acta Cryst. C* **2015**, *71*, 3-8.
3. CrysAlisPro, 1.171.38.41; Rigaku Americas Corporation: The Woodlands, TX, 2015.
4. Frisch, M. J.; Trucks, G. W.; Schlegel, H. B.; Scuseria, G. E.; Robb, M. A.; Cheeseman, J. R.; Scalmani, G.; Barone, V.; Mennucci, B.; Petersson, G. A.; Nakatsuji, H.; Caricato, M.; Li, X.; Hratchian, H. P.; Izmaylov, A. F.; Bloino, J.; Zheng, G.; Sonnenberg, J. L.; Hada, M.; Ehara, M.; Toyota, K.; Fukuda, R.; Hasegawa, J.; Ishida, M.; Nakajima, T.; Honda, Y.; Kitao, O.; Nakai, H.; Vreven, T.; Montgomery, J. A.; Peralta, J. E.; Ogliaro, F.; Bearpark, M.; Heyd, J. J.; Brothers, E.; Kudin, K. N.; Staroverov, V. N.; Kobayashi, R.; Normand, J.; Raghavachari, K.; Rendell, A.; Burant, J. C.; Iyengar, S. S.; Tomasi, J.; Cossi, M.; Rega, N.; Millam, J. M.; Klene, M.; Knox, J. E.; Cross, J. B.; Bakken, V.; Adamo, C.; Jaramillo, J.; Gomperts, R.; Stratmann, R. E.; Yazev, O.; Austin, A. J.; Cammi, R.; Pomelli, C.; Ochterski, J. W.; Martin, R. L.; Morokuma, K.; Zakrzewski, V. G.; Voth, G. A.; Salvador, P.; Dannenberg, J. J.; Dapprich, S.; Daniels, A. D.; Farkas; Foresman, J. B.; Ortiz, J. V.; Cioslowski, J.; Fox, D. J. Gaussian 09, Revision B.01. Wallingford CT **2009**.
5. Fujisawa, K.; Soma, S.; Kurihara, H.; Dong, H. T.; Bilodeau, M.; Lehnert, N. A. *Dalton Trans.* **2017**, *46*, 13273-13289.
6. Dong, H. T.; White, C. J.; Zhang, B.; Krebs, C.; Lehnert, N. *J. Am. Chem. Soc.* **2018**, *140*, 13429-13440.
7. Wang, J.; Li, C.; Zhou, Q.; Wang, W.; Hou, Y.; Zhang, B.; Wang, X. *Dalton Trans.* **2016**, *45*, 5439-5443.
8. Wong, Y.-L.; Mak, C.-Y.; Kwan, H. S.; Lee, H. K. *Inorg. Chim. Acta* **2010**, *363*, 1246-1253.
9. Diebold, A.; Hagen, K. S. *Inorg. Chem.* **1998**, *37*, 215-223.
10. Berto, T. C.; Hoffman, M. B.; Murata, Y.; Landenberger, K. B.; Alp, E. E.; Zhao, J.; Lehnert, N. *J. Am. Chem. Soc.* **2011**, *133*, 16714-16717.
11. Zheng, S.; Berto, T. C.; Dahl, E. W.; Hoffman, M. B.; Speelman A. L.; Lehnert, N. *J. Am. Chem. Soc.* **2013**, *135*, 4902-4905.